

A Primer on Partial Wave Analysis

K. PETERS

*Institut für Experimentalphysik,
Ruhr-Universität Bochum,
D-44780 Bochum, Germany*

Summary. — In the 90s of the last century high statistics experiments with fully equipped 4π detectors have lead to a better insight in the spectrum of hadrons. In particular the finding of crypto-exotic and J^{PC} exotic states tremendously improved the experimental situation in meson spectroscopy. All this was possible only with sophisticated analysis methods like the decomposition of measured phase-space distribution into partial waves and to express the partial waves in terms of complicated dynamical functions. This paper gives an introduction about the concepts and formalisms involved.

PACS 11.80 – Partial wave analysis.

1. – Introduction

1.1. Goals. – The spectrum of hadrons, mesons and baryons is the result of bound states of quarks like $q\bar{q}$ and qqq respectively. Although the quark-model was motivated partly by the structure of the spectra and the symmetry and decay properties of the hadrons, the gauge field theory of strong interactions, Quantum Chromodynamics (QCD), has a very strong coupling constant at very low momentum transfer (e.g. low masses) so that there are no firm predictions in the classical field of light quark spectroscopy and medium energy physics. Therefore there is no possibility to map out the

states from first principles (if we leave lattice gauge theory out for the moment). To understand the spectrum of light hadrons it is important to collect the properties to derive effective models to be used in that field, which may tie up to the very high energies where perturbative QCD works well. In order to uncover the spectrum it is necessary to investigate the scattering and the decay of hadrons and to identify the intermediate states throughout the whole reaction.

Lattice gauge theory could be a way out of the problem, but since the results reflect a measurement on the lattice (with very limited precision and a lot of assumptions so far) it is not suited to actually understand the principles and the physics behind the measurements, e.g. an actual state and/or its properties.

The basic task is to find all resonances, with their static properties like mass, width, spin and parities. Since $SU_F(3)$ [1] provides a lot of relations among the decays of pure states (without Fock states) without complicated final state effects it is important to measure the partial decays widths as well. This is a very demanding task, since a lot of resonances overlap. In addition complicated production processes or scattering with many waves in the intermediate state complicate the situation. To disentangle the waves and to identify resonances and their actual yield.

1.2. Technique. – The techniques are manifold and we should concentrate only on two basic approaches. The first one is scattering of hadrons, usually on a proton or a deuterium target, depending on the desired process. Typical examples are

- πN scattering with or without charge exchange (GAMS at CERN, E852 at AGS),
- γN scattering (CEBAF, MAMI, Elsa, Graal),
- πp or pp in the central region (WA76, WA92, WA102 at CERN, E690 at FNAL),
- pp near meson production thresholds (WASA at Celsius, Anke and TOF at COSY),
- $\bar{p}p$ in flight (Crystal barrel, Jetset and PS185 at CERN, Panda at GSI).

These reactions involve usually a lot of partial waves. Single or double polarization experiments, low excitation energies and/or a selection of specific exclusive channels which impose reasonable constraints on the reaction are required to enable an unambiguous decomposition of the system.

The second one is where the initial system is at rest and/or the remaining part of the reaction is not of interest like

- $\bar{p}N$ reactions at rest into many body final states (Asterix, Crystal barrel and Obelix at LEAR),
- K^0 and K^\pm decays (NA48 at CERN, Kloe at Da ϕ ne, kTev at FNAL),
- $\phi(1020)$ decays (Kloe at Da ϕ ne, VEPP at Novosibirsk),
- D and D_s decays in high energy reactions (photo-production at FNAL, Babar/Belle at PEP-2/KEK-B, CLEO-c at CESR),

- J/ψ decays (MarkIII at SLAC, DM2, CLEO-c at CESR, BES at BEPC).

For all experiments of this type it is important that spin densities are well known. Otherwise a full decomposition is not possible. In that case additional assumptions have to be made to relate the different parameters.

1.3. Methods. –

1.3.1. The Partial Wave Approach.

Motivation. Partial waves are easily introduced in a scattering process. To get a first impression we start with Schrödinger's equation

$$(1) \quad -\frac{\hbar}{2\mu} \nabla^2 \Psi(\vec{r}) + V(\vec{r})\Psi(\vec{r}) = E\Psi(\vec{r})$$

with $\vec{k} = \frac{\vec{p}}{\hbar} = \mu \frac{\vec{v}}{\hbar}$ and the reduced mass $\mu = \frac{m_1 m_2}{m_1 + m_2}$. The incident wave can be expressed like $\Psi_i(r, \vartheta, \varphi) = e^{ikz}$ and we assume a vanishing potential $V(\vec{r}) = 0$. Then we can expand the initial state $|i\rangle$ in terms of Legendre polynomials P_l , thus separating angular and radial wave function

$$(2) \quad |i\rangle = \Psi_i = \sum_{l=0}^{\infty} U_l(r) P_l(\cos \vartheta).$$

The scattering wave function Ψ_S is the difference between incoming and outgoing wave. We parametrize U_l in terms of a phase δ_l and an inelasticity η_l , which are motivated from our knowledge of resonance curves, where the phase moves from $-\frac{\pi}{2}$ to $\frac{\pi}{2}$ and the inelasticity carries all dissipated probability (e.g. into other channels):

$$(3) \quad \Psi_S = \Psi_f - \Psi_i = \frac{1}{k} \sum_{l=0}^{\infty} (2l+1) \frac{\eta_l e^{2i\delta_l} - 1}{2i} P_l(\cos \vartheta) \frac{e^{ikr}}{r}$$

The total cross section can then be written

$$(4) \quad \begin{aligned} \frac{d\sigma}{d\varphi d\cos\vartheta} &= \frac{1}{k^2} \left| \sum_{l=0}^{\infty} (2l+1) \frac{\eta_l e^{2i\delta_l} - 1}{2i} P_l(\cos \vartheta) \right|^2 \\ &= \frac{1}{k^2} \left| \sum_{l=0}^{\infty} (2l+1) T_l P_l(\cos \vartheta) \right|^2 \end{aligned}$$

with

$$(5) \quad T_l = \frac{\eta_l e^{2i\delta_l} - 1}{2i}$$

the so called T -matrix. We will discuss it's properties later in more detail (see sec. 3.2.4). To visualize the properties of T Argand plots are quite useful, since they provide a check on the unitarity of T (which ensures that the probability of a reaction does not exceed unity). The Argand plot is a graph of the imaginary part of T versus the real part of T (see fig. 1). It is seen easily from this plot that the phase δ_l is not the same as the angle ϕ which appears in the polar representation of complex numbers. As an example,

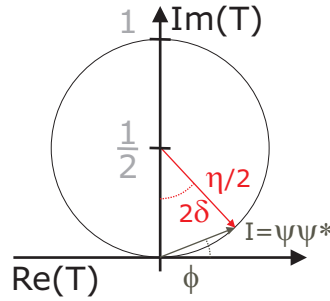


Fig. 1. – Argand plot definitions.

fig. 2 shows the behavior of T for a relativistic Breit-Wigner function. If the inelasticity is zero, e.g. there is only one elastic channel, the Argand circle has a constant radius of $\frac{1}{2}$ and crosses the imaginary axis at one. From eq. 4 we see that the angular amplitudes (P_l) and the dynamic amplitude (T_l) factorize.

1.3.2. The Isobar Model. The last preparative step to write down an amplitude is to make assumptions how particles are grouped to construct a decay/reaction chain. An empirical approach is the isobar model. It assumes that all subsequent decays appear to be two-body reactions. This model seems to work extremely well in very different environments and for most hadrons (exceptions may be $\omega \rightarrow \pi^+ \pi^- \pi^0$ and $\eta \rightarrow 3\pi$). The type of valid reactions is sketched in fig. 3a while fig. 3b shows a more complicated reaction involving rescattering. The isobar approach will not work easily in those circumstances. In some cases it can be retained if the rescattering process is refactorizable in terms of many isobar reactions. This involves usually very many parameters and may not lead to a sufficient description. In those cases model assumptions have to be made. In the isobar model, the two-body decay into particle 1 and 2 factorizes (fig. 4) completely from the recoil system 3, which might decay as well. Any node in the decay tree is represented by the same isobar-like amplitude. The recoil systems are only involved in maintaining the conservation of angular momentum and spin-projections, which imply summation over unobservable quantities.

1.3.3. Construction of the Amplitude. The full amplitude for each node of the decay tree consists of a dynamical part T_l and an angular part which we will call R_l . If we deal with strong or electromagnetic interactions also isospin is conserved, which means that we have to include an isospin related part I_l , so that decays with different isospins

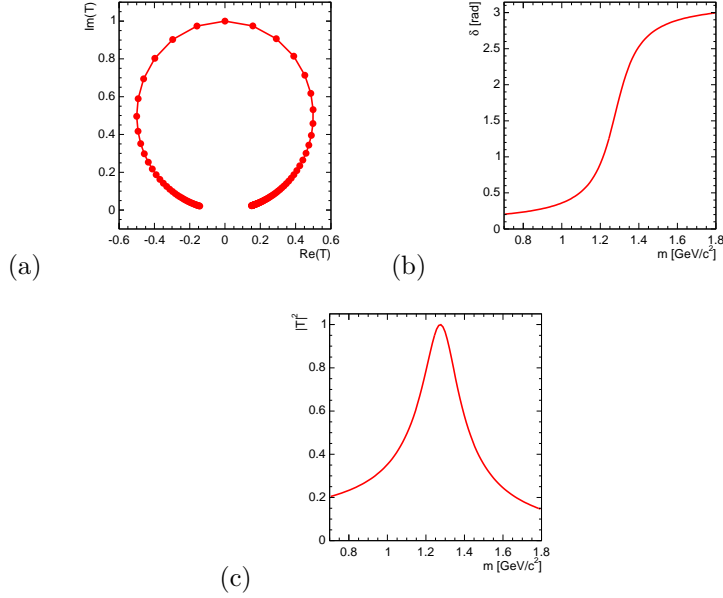


Fig. 2. – Simple relativistic Breit-Wigner. (a) Argand, (b) phase δ and (c) intensity plot.

$|II_3\rangle$ can be related to each other. This is important if the same charged particle occur with different charge in various parts of the decay tree. With these ingredients, the full amplitude is defined via

$$(6) \quad f(I, I_3, s, \Omega) = I_l(I, I_3)T_l(s)R_l(\Omega)$$

One should note, that after combining the amplitude for all nodes in the decay tree, all conservation laws (like J , I , and their respective projections) have to be taken into account, which results in a sum over all unobservable values.

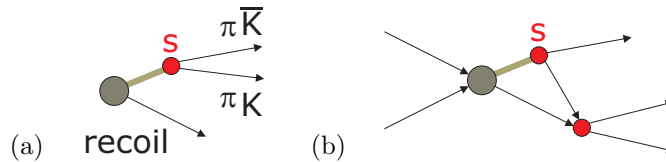


Fig. 3. – Production process with propagation (a) and rescattering (b). (a) can be treated easily with an isobar method, while (b) can not.

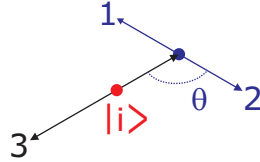


Fig. 4. – Isobar definition in a chain of subsequent decays. θ defines the angle for angular decay distributions.

Example: Isospin Relations in $\bar{p}p(0^{-+}, 1^{--}) \rightarrow \rho\pi$. The initial $\bar{p}p$ state has either $I^G(J^{PC}) = 1^-(0^{-+})$ (called 1S_0) or $I^G(J^{PC}) = 0^-(1^{--})$ (called 3S_1). The two final state gammas have $I^G(J^{PC}) = 0^+(1^{--})$. Both initial states can decay to $\rho\pi$ but this case illustrates how important isospin Clebsch-Gordan coefficients are, since

$$\begin{aligned}
 \rho^0\pi^0 &\rightarrow (1010|00) = -\sqrt{\frac{1}{3}} \\
 \rho^0\pi^0 &\rightarrow (1010|10) = 0 \\
 \rho^\pm\pi^\mp &\rightarrow (1(\pm 1) 1(\mp 1)|00) = \sqrt{\frac{1}{3}} \\
 \rho^\pm\pi^\mp &\rightarrow (1(\pm 1) 1(\mp 1)|10) = \pm\sqrt{\frac{1}{2}}
 \end{aligned}
 \tag{7}$$

it is evident that 1S_0 has destructive $\rho^\pm/\rho^0\pi^0$ interference, while for 3S_1 only $\rho^\pm\pi^\mp$ contributes and $\rho^0\pi^0$ does not exist.

2. – Spin formalisms

2.1. Preface. – There are various spin formalisms available. In principle there are three basic types:

- tensor formalisms, in non-relativistic (Zemach) or covariant form,
- spin-projection formalisms, where a quantization axis is chosen and proper rotations are used to define a two-body decay
- formalisms based on Lorentz invariants (Rarita-Schwinger) where each operator is constructed from Mandelstam variables only.

The tensor formalisms are very fast algorithms if waves with small angular momentum are involved but is getting very complicated if higher waves are present and/or a lot of subsequent decays occur. Using the Lorentz invariants is not really a formalism, since one has to construct an amplitude with the proper transformation and symmetry properties as the actual particle and wave to be represented. As for the tensor formalism this might be simple and extremely elegant for waves with low angular momentum but is virtually

impossible for a complicated decay cascade. The Zemach formalism as a representative of tensor formalisms is discussed in sec. 2.2.

If we restrict ourselves now to the other formalisms the key steps in the specification of a scattering formalism are as follows:

- the definition of single particle states of given momentum and spin component (\vec{p} -states),
- the definition of two-particle \vec{p} -states in the s -channel center-of-mass system and of amplitudes between them,
- transformation to states and amplitudes of given total angular momentum (J -states),
- symmetry restrictions on the amplitudes,
- formulae for observable quantities,
- specification of kinematic constraints.

The basic three formalisms are known as helicity, transversity and canonical (historically known as orbital) formalisms. Their basic properties are summarized in tbl. I. Since they have different symmetry relations they can be used in different fields. While the helicity formalism is applicable to most spectroscopy experiment, it is the transversity formalism which conserves parity and can therefore be applied for partial wave decomposition in CP measurements. The three formalisms differ mainly in the choice of the spin quantization

property	Helicity	Transversity possible/simplicity	Canonical (Orbital)
partial wave expansion	simple	complicated	complicated
parity conservation	no	yes	yes
crossing relation	no	good	bad
specification of kinematic constraints	no	yes	yes

TABLE I. – *Comparison of various spin formalisms. Depending on the choice of the quantization axis, the amplitudes have different symmetry properties.*

direction for each particle.

In the helicity formalism each particle spin is quantized parallel to its own direction of motion so that its projection, the helicity λ is diagonal.

In the transversity approach, the component τ normal to the scattering plane is used.

In the orbital (or canonical approach) the component m in the incident z -direction is diagonal.

The merits of each approach arise largely from the invariance of the projections. These properties are made precise by the definition of the particle states. It is convenient to define them by explicit Lorentz transformation from the spin states m of a particle at rest.

Detailed discussions are found in the original papers [2, 3, 4]. The essential principle in all cases is, that the spin projection of a particle is defined in its rest frame. The general single particle state is then defined by applying a definite sequence of boosts $L(p_x, p_y, p_z)$ and rotation $R(\alpha, \beta, \gamma)$ to the system. We define

$$(8) \quad \Psi_\lambda = |\tilde{p}, \lambda\rangle = \widehat{R}(\phi, \theta, -\phi)\widehat{B}(0, 0, p)|m\rangle \equiv \widehat{H}(\tilde{p})|\lambda\rangle$$

$$(9) \quad \Psi_\tau = |\tilde{p}, \tau\rangle = \sum_\lambda |\tilde{p}, \lambda\rangle \Delta_{\lambda\tau}^J = \widehat{\Delta}\widehat{H}(\tilde{p})\widehat{\Delta}^{-1}|\tau\rangle = \widehat{T}|\tau\rangle$$

$$(10) \quad \Psi_m = |\tilde{p}m\rangle = \sum_\lambda |\tilde{p}, \lambda\rangle D_{\lambda\tau}^{J*} \widehat{R}(\phi, \theta, -\phi) = \widehat{R}^{-1}(\phi, \theta, -\phi)\widehat{H}(\tilde{p})|m\rangle = \widehat{O}|m\rangle.$$

It is clear that it is necessary to calculate the effect of a general Lorentz transformation on the states $|\tilde{p}\xi\rangle$. While $L\tilde{p} = \tilde{p}'$ the corresponding state is not $|\tilde{p}', \xi\rangle$ since the states are being always obtained from the rest state by a definite sequence $X(\tilde{p})$ and these do not in general commute. However, since both have the same value for the momentum in a particular system they can both be transformed back to the rest frame by X^{-1} can there they can differ at most by a rotation

$$(11) \quad L|\tilde{p}\xi\rangle = X(L\tilde{p})R(L, \tilde{p})|0\xi\rangle = \sum_{\xi'} |L\tilde{p}, \xi'\rangle D_{\xi'\xi}^J(r)$$

with the Wigner rotation given by

$$(12) \quad R = X^{-1}(L\tilde{p})LX(\tilde{p}).$$

The two-particle states are then defined essentially as direct products of single particle states, but phase space factors may be included to make the form in the center-of-mass system convenient for various purposes. More details are discussed in the particular sections about the different formalisms (see sec. 2'3.1).

2'2. Zemach Formalism. –

2'2.1. Formalism. The Zemach formalism was originally developed for the investigation of the K^0 decays into 3π [5]. The basic concept is that every angular momentum involved in the reaction is represented by a symmetric and traceless tensor of rank l in 3-dim. phase-space. The tensors A for spins up to two are

$$(13) \quad \begin{aligned} l = 0 & \quad A^0 = 1 \\ l = 1 & \quad A^1(\vec{q}) = \vec{q} \\ l = 2 & \quad A^2(\vec{q}) = \frac{3}{2} \left[\vec{q} \cdot \vec{q}^T - \underbrace{\frac{1}{3}|\vec{q}|^2}_{\text{for tracelessness}} \right] \end{aligned}$$

with

$$(14) \quad \vec{q} \cdot \vec{p}^T = \begin{pmatrix} q_1 \\ q_2 \\ q_3 \end{pmatrix} \begin{pmatrix} p_1 & p_2 & p_3 \end{pmatrix} = \begin{pmatrix} q_1 p_1 & q_1 p_2 & q_1 p_3 \\ q_2 p_1 & q_2 p_2 & q_2 p_3 \\ q_3 p_1 & q_3 p_2 & q_3 p_3 \end{pmatrix}$$

or with all indices

$$(15) \quad \begin{aligned} l = 0 & \quad A^0 = 1 \\ l = 1 & \quad A_i^1 = q_i \\ l = 2 & \quad A_{ij}^2 = \frac{3}{2} q_i q_j - \frac{1}{2} |q_i|^2 \delta_{ij}. \end{aligned}$$

The coupling of spins and/or angular momenta, like spin s of a particle and angular momentum l relative to another spinless particle is then done by multiplying the tensors and contraction of the resulting tensor.

2.2.2. Example: $\bar{p}p(0^{-+}) \rightarrow f_2 \pi^0 \rightarrow \pi^+ \pi^- \pi^0$. The two step process $\bar{p}p \rightarrow f_2 \pi^0$ and $f_2 \rightarrow \pi^+ \pi^-$ may serve as an example to illustrate the method. For \vec{p} being the momentum between π^0 and f_2 and \vec{q} the momentum in the subsequent $f_2 \rightarrow \pi^+ \pi^-$ two-body decay the construction of the amplitude leads to

$$(16) \quad \begin{aligned} A^0 &= A_{f_2 \pi^0, ij}^2 A_{\pi^+ \pi^-, kl}^2 \underbrace{\delta_{ik} \delta_{jl}}_{\text{unpolarized}} \\ &= \sum_{i,j,k,l} A_{f_2 \pi^0, ij}^2 A_{\pi^+ \pi^-, kl}^2 \delta_{ik} \delta_{jl} \\ &= \sum_{i,j} A_{f_2 \pi^0, ij}^2 A_{\pi^+ \pi^-, ij}^2 \end{aligned}$$

with

$$(17) \quad A_{f_2 \pi^0, ij}^2 = \frac{3}{2} p_i p_j - \frac{1}{2} |p_i|^2 \delta_{ij}$$

$$(18) \quad A_{\pi^+ \pi^-, kl}^2 = \frac{3}{2} q_k q_l - \frac{1}{2} |q_l|^2 \delta_{kl}.$$

Combining eq. 18 and eq. 17 with eq. 16 gives

$$(19) \quad \begin{aligned} A^0 &= \left(\frac{3}{2} p_i p_j - \frac{1}{2} |p_i|^2 \delta_{ij} \right) \left(\frac{3}{2} q_i q_j - \frac{1}{2} |q_i|^2 \delta_{ij} \right) \\ &= \frac{9}{4} (\vec{q} \cdot \vec{p})^2 - \frac{3}{4} \vec{q}^2 \vec{p}^2 - \frac{3}{4} \vec{q}^2 \vec{p}^2 + 3 \frac{1}{4} |\vec{q}|^2 |\vec{p}|^2 \\ &= \frac{9}{4} (\vec{q} \cdot \vec{p})^2 - \frac{3}{4} \vec{q}^2 \vec{p}^2 \end{aligned}$$

and finally the angular distribution is calculated by the squared amplitude

$$(20) \quad \frac{9}{4} \left[(\vec{q} \cdot \vec{p})^2 - \frac{1}{3} q^2 p^2 \right] = \frac{9}{4} \left[(qp \cos \vartheta)^2 - \frac{1}{3} q^2 p^2 \right] \\ = \frac{9}{4} \left(\cos^2 \vartheta - \frac{1}{3} \right)^2 = P_2^0(\vartheta)^2.$$

2.3. Canonical and Helicity Formalism. –

2.3.1. Few Particle States.

Canonical (Orbital) Formalism.

Single Particle States May $|jm\rangle$ be an at-rest state with spin j and spin projection m on to the z -axis in an euclidean system with coordinates (x, y, z) . The single particle state with a momentum \vec{p} is constructed through a pure Lorentz transformation $L_{\vec{p}}$

$$(21) \quad |\vec{p}, jm\rangle \stackrel{def}{=} L_{\vec{p}} |jm\rangle \\ = \widehat{R}_0 L_z p \widehat{R}_0^{-1} |jm\rangle$$

where $\widehat{R}_0 = \widehat{R}_0(\varphi, \vartheta, 0)$ rotates the z -axis (like in fig. 5a) in the direction of the momentum \vec{p} ($\vec{e}_{\vec{p}} = \widehat{R}_0(\varphi, \vartheta, 0)\vec{e}_z$). In the first step the momentum vector is rotated via \widehat{R}_0^{-1} in the

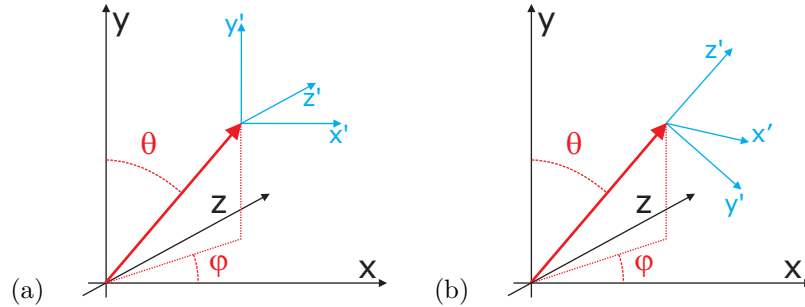


Fig. 5. – Definition of angles in canonical (a) and helicity formalism (b).

z -direction. Secondly the absolute value of the momentum is Lorentz transformed along z and finally the z -axis is rotated to the \vec{p} direction via \widehat{R}_0 .

If rotation of the single particle state is derived from the properties of the rotation group. One obtains

$$(22) \quad \widehat{R} |\vec{p}, m\rangle = \sum_{m'} D_{m'm}^j(\widehat{R}) |\vec{p}, m'\rangle$$

where $D_{m'm}^j(R)$ are the Wigner D -functions for the rotation R . From eq. 22 we see that the canonical states transform like at-rest states $|jm\rangle$.

Two-Particle States Two-particle systems 1+2 in a rest-system J with respective spins can be constructed directly with the help of single particle states. One particle s has the momentum \vec{p}_s and the other particle t has the opposite momentum $-\vec{p}_s$. Apart from that the at-rest system of the two particles depends only on the stereo angle Ω_s and the direction of \vec{p}_s . Using eq. 21 one gets

$$(23) \quad |\Omega_s^0, sm_s tm_t\rangle \stackrel{def}{=} \kappa \left[L \underbrace{\tilde{p}_s}_{(E_s, \tilde{p}_s)} |sm_s\rangle L \underbrace{\tilde{p}_t}_{(E_t, -\tilde{p}_s)} |tm_t\rangle \right].$$

The normalization κ can be derived from the single particle states:

$$(24) \quad \kappa = \frac{1}{4\pi} \sqrt{\frac{p_s}{m_J}} = \frac{1}{4\pi} \sqrt{\rho_s}$$

where m_J is the invariant mass of the state J and ρ_s the invariant phase-space factor.

To get a practical recipe it is necessary to couple the angular momentum L and the total spin $S = s + t$. Thus the first step is the coupling of the single particle spins to S

$$(25) \quad |\Omega, Sm_S\rangle = \sum_{m_s, m_t} (sm_s tm_t | Sm_S) |\Omega, sm_s tm_t\rangle$$

where $(sm_s tm_t | Sm_S)$ is a Clebsch-Gordan coefficient. A state with a particular total angular momentum L is then

$$(26) \quad |Lm_L Sm_S\rangle = \int d\Omega Y_{m_L}^L(\Omega) |\Omega, Sm_S\rangle$$

Finally we couple L and S to J :

$$(27) \quad \begin{aligned} |JM LS\rangle &= \sum_{m_L, m_S} (Lm_L Sm_S | JM) |Lm_L Sm_S\rangle \\ &= \sum_{m_L, m_S, m_s, m_t} (Lm_L Sm_S | JM) (sm_s tm_t | Sm_S) \int \Omega Y_{m_L}^L(\Omega) |\Omega_s^0, sm_s tm_t\rangle \end{aligned}$$

with $Y_{m_L}^L(\Omega)$ being the spherical harmonics. With these definitions we get the following completeness relation

$$(28) \quad 1 = \sum_{J, M, L, S} |JM LS\rangle \langle JM LS|.$$

The normalization of the canonical states is then given by

$$(29) \quad \langle \Omega_{s'}, s' m_{s'} t' m_{t'} | \Omega_s, sm_s tm_t \rangle = \delta(\Omega_{s'} - \Omega_s) \delta_{s s'} \delta_{t t'} \delta_{m_s m_{s'}} \delta_{m_t m_{t'}}$$

$$(30) \quad \langle J' M' L' S' | JM LS \rangle = \delta_{J J'} \delta_{M M'} \delta_{L L'} \delta_{S S'}.$$

Helicity Formalism.

Single Particle States The construction of states is similar to the procedure for canonical states. May $|j\lambda\rangle$ be an at-rest state with spin j and spin projection λ on to the z -axis in an euclidean system with coordinates (x, y, z) . The single particle state with a momentum \vec{p} is constructed through a pure Lorentz transformation $L\tilde{p}$ plus a rotation. This is due to the fact, that the z -axis is firstly rotated to the direction of \vec{p} . Secondly the result is Lorentz transformed. Therefore the new z -axis, z' , is parallel to \vec{p} (see fig. 5b).

$$(31) \quad |\vec{p}, j\lambda\rangle \stackrel{def}{=} L\tilde{p}|j\lambda\rangle$$

$$(32) \quad = \widehat{R}_0 L_z p \widehat{R}_0^{-1} |j\lambda\rangle.$$

The second line of eq. 31 follows from eq. 21 and the unitarity of rotations. If the helicity state is rotated, then the momentum \vec{p} is rotated, but the helicity is invariant, since the quantization axis is rotated as well. Therefore

$$(33) \quad \widehat{R}|\vec{p}, \lambda\rangle = |\widehat{R}\vec{p}, \lambda\rangle.$$

Since eq. 22 and 33 are complete, it is possible to represent the helicity state in the canonical basis and vice versa:

$$(34) \quad |\vec{p}, \lambda\rangle = \sum_m D_{m\lambda}^j(R_0) |\vec{p}, m\rangle$$

Two-Particle States Analogue to the construction of the canonical two-particle state eq. 21, the helicity equivalent is constructed using the states eq. 31

$$(35) \quad |\Omega_s, s\lambda_s t\lambda_t\rangle \stackrel{def}{=} \kappa \widehat{R}_0 [L_z p_s |s\lambda_s\rangle L_z p_t |t\lambda_t\rangle]$$

$$= \widehat{R}_0(\Omega_s) |\Omega = (0, 0), s\lambda_s t\lambda_t\rangle$$

Using a similar procedure to couple all spins one obtains

$$(36) \quad |JM\lambda_s\lambda_t\rangle = N_J \int d\Omega \quad D_{M, \lambda_s - \lambda_t}^{J*} |\Omega, s\lambda_s t\lambda_t\rangle$$

with the normalization factor

$$(37) \quad N_J = \sqrt{\frac{2J+1}{4\pi}}.$$

The choice of N_J was made, so that we get a simple completeness relation

$$(38) \quad 1 = \sum_{J, M, \lambda_s, \lambda_t} |JM\lambda_s\lambda_t\rangle \langle JM\lambda_s\lambda_t|$$

The normalization of the helicity states is then given by

$$(39) \quad \langle \Omega_{s'}, s' \lambda_{s'} t' \lambda_{t'} | \Omega_s, s \lambda_s t \lambda_t \rangle = \delta(\Omega_{s'} - \Omega_s) \delta_{ss'} \delta_{tt'} \delta_{\lambda_s \lambda_{s'}} \delta_{\lambda_t \lambda_{t'}}$$

$$(40) \quad \langle J' M' \lambda_{s'} \lambda_{t'} | J M \lambda_s \lambda_t \rangle = \delta_{JJ'} \delta_{MM'} \delta_{\lambda_s \lambda_{s'}} \delta_{\lambda_t \lambda_{t'}}$$

2.3.2. Decay Amplitudes. The two-particle states can now be used to derive two-body decay formulae in the two formalisms.

Canonical (Orbital) Formalism. May J be the at-rest system of the decaying state $|JM\rangle$ with arbitrary, but well defined spin J and projection M . The decay amplitudes is derived by using the two-particle states and summing over all unobservable spin-projections

$$(41) \quad A = \sum_{m_s, m_t} \langle \vec{p}_s, sm_s | \langle -\vec{p}_s, tm_t | \mathcal{M} | JM \rangle$$

with \mathcal{M} being the unknown decay operator. To get to the final formula we need the following relation

$$(42) \quad \begin{aligned} \langle \Omega_s, sm_s tm_t | JMLS \rangle &= \sum_{m_L, m_S, m_{s'}, m_{t'}} (Lm_L Sm_S | JM) (s' m_{s'} t' m_{t'} | Sm_S) \\ &\int d\Omega_{s'} Y_{m_L}^L(\Omega_{s'}) \langle \Omega_s, sm_s tm_t | \Omega_{s'}, s' m_{s'} t' m_{t'} \rangle \end{aligned}$$

$$(43) \quad \begin{aligned} &= \sum_{m_L, m_S, m_{s'}, m_{t'}} (Lm_L Sm_S | JM) (s' m_{s'} t' m_{t'} | Sm_S) \\ &\int d\Omega_{s'} \delta(\Omega_s - \Omega_{s'}) \delta_{ss'} \delta_{tt'} \delta_{m_s m_{s'}} \delta_{m_t m_{t'}} \\ &= \sum_{m_L, m_L} (Lm_L Sm_S | JM) (sm_s tm_t | Sm_S) Y_{m_L}^L(\Omega_s) \end{aligned}$$

Now we include the two-particle states and obtain

$$(44) \quad \begin{aligned} A_{m_s m_t}^{JM} &= \frac{4\pi}{\sqrt{\rho_s}} \langle \Omega_s, sm_s tm_t | \mathcal{M} | JM \rangle \\ &= \sum_{L, S} \langle \Omega_s, sm_s tm_t | JMLS \rangle \frac{4\pi}{\sqrt{\rho_s}} \langle JMLS | \mathcal{M} | JM \rangle \end{aligned}$$

$$(45) \quad \begin{aligned} &\stackrel{def}{=} \sum_{L, S} \sqrt{4\pi} a_{LS}^J \langle \Omega_s, sm_s tm_t | JMLS \rangle \\ &\stackrel{def}{=} \sum_{L, S, m_L, m_S} \sqrt{4\pi} a_{LS}^J (Lm_L Sm_S | JM) (sm_s tm_t | Sm_S) Y_{m_L}^L(\Omega_s) \end{aligned}$$

with the canonical partial decay amplitudes a_{LS}^J

$$(46) \quad a_{LS}^J \stackrel{def}{=} \sqrt{\frac{4\pi}{\rho_s}} \langle JMLS | \mathcal{M} | JM \rangle$$

which contain the physical matrix element of operator \mathcal{M} .

Helicity Formalism. The decay helicity amplitude is derived in the same way as eq. 41

$$(47) \quad A = \sum_{\lambda_s, \lambda_t} \langle \vec{p}_s, s\lambda_s | \langle -\vec{p}_s, t\lambda_t | \mathcal{M} | JM \rangle.$$

Using

$$(48) \quad \begin{aligned} \langle \Omega_s, s\lambda_s t\lambda_t | JM \lambda_{s'} \lambda_{t'} \rangle &= N_J \int d\Omega' D_{M, \lambda_{s'} - \lambda_{t'}}^{J*}(\Omega') \langle \Omega_s, s\lambda_s t\lambda_t | \Omega_{s'}, s' \lambda_{s'} t' \lambda_{t'} \rangle \\ &= N_J \int d\Omega_{s'} D_{M, \lambda_{s'} - \lambda_{t'}}^{J*}(\Omega_{s'}) \delta(\Omega_{s'} - \Omega_s) \delta_{s s'} \delta_{t t'} \delta_{\lambda_s \lambda_{s'}} \\ &= N_J D_{M, \lambda_{s'} - \lambda_{t'}}^{J*}(\Omega_s) \end{aligned}$$

and inserting the two-particle states we get

$$(49) \quad \begin{aligned} A_{\lambda_s \lambda_t}^{JM} &= \frac{4\pi}{\rho_s} \langle \Omega_s, s\lambda_s t\lambda_t | \mathcal{M} | JM \rangle \\ &= \sum_{\lambda_{s'}, \lambda_{t'}} \langle \Omega_s, s\lambda_s t\lambda_t | JM \lambda_{s'} m_{t'} \rangle \frac{4\pi}{\rho_s} \langle JM \lambda_{s'} m_{t'} | \mathcal{M} | JM \rangle \\ &= \sqrt{\frac{4\pi}{\rho_s}} (2J+1) \langle JM \lambda_s m_t | \mathcal{M} | JM \rangle D_{M, \lambda_{s'} - \lambda_{t'}}^{J*}(\Omega_s) \\ (50) \quad &= N_J f_{\lambda_s \lambda_t} D_{M, \lambda_{s'} - \lambda_{t'}}^{J*}(\Omega_s) \end{aligned}$$

with the helicity amplitudes

$$(51) \quad N_J f_{\lambda_s \lambda_t} = \sqrt{\frac{4\pi}{\rho_s}} (2J+1) \langle JM \lambda_s m_t | \mathcal{M} | JM \rangle$$

also containing the physical matrix element of operator \mathcal{M} . The two formulae eq. 45 and eq. 50 have a lot of similarities. They are both an expansion in terms of spherical functions of different type ($Y_{m_L}^L$ for the canonical and $D_{m' m}^J$ for the helicity formalism) with partial amplitudes which cover the decay matrix element.

To obtain an intensity it is necessary to include the population of spin states of the initial state. For a particle with spin J there are $2J+1$ projections to the quantization axis, thus leading to a spin-density matrix ρ of rank $2J+1$ which is usually diagonal and has the form

$$(52) \quad \rho_{MM'} = \begin{pmatrix} 1 & & 0 \\ & \ddots & \\ 0 & & 1 \end{pmatrix}$$

With this definition the observed number of events is given by

$$(53) \quad I(\vartheta)_{\lambda\lambda'} = \sum_{M, M', \lambda_s, \lambda_{s'}, \lambda_t, \lambda_{t'}} A_{\lambda_s \lambda_t}^{JM}(\varphi, \vartheta) \rho_{MM'} A_{\lambda_{s'} \lambda_{t'}}^{JM'*}(\varphi, \vartheta)$$

where the summation over $\lambda_s, \lambda_{s'}, \lambda_t, \lambda_{t'}$ is implicitly constrained to $\lambda = \lambda_s - \lambda_t$ and $\lambda' = \lambda_{s'} - \lambda_{t'}$

2.3.3. Relations between Canonical and Helicity Base. Since both approaches deliver a complete description of the state, it is fairly easy to go from one representation to another. This is important if L and S are good quantum numbers for the system. Then the recoupling coefficients lead to symmetry relations among the helicity amplitudes.

To move from one representation to the other we need the recoupling coefficients. They are derived using the properties of the D -functions:

$$(54) \quad \langle JM|LS|JM\lambda_s\lambda_t\rangle = \sqrt{\frac{2L+1}{2J+1}} (L0\ S(\lambda_s - \lambda_t)|J(\lambda_s - \lambda_t))(s\lambda_s\ t(-\lambda_t)|S(\lambda_s - \lambda_t))$$

With eq. 54 we obtain a relation between $f_{\lambda_s\lambda_t}$ and a_{LS}^J . The recoupling from the canonical to the helicity representation is

$$(55) \quad \begin{aligned} N_J f_{\lambda_s\lambda_t}^J &= \sum_{L,S} \langle JM\lambda_s\lambda_t|JMLS\rangle \sqrt{\frac{4\pi}{\rho_s}} (2J+1) \langle JMLS|\mathcal{M}|JM\rangle \\ &= \sum_{L,S} \sqrt{2L+1} (L0\ S(\lambda_s - \lambda_t)|J(\lambda_s - \lambda_t))(s\lambda_s\ t(-\lambda_t)|S(\lambda_s - \lambda_t)) a_{LS}^J \end{aligned}$$

while from the helicity to the canonical representation is

$$(56) \quad \begin{aligned} a_{LS}^J &= \sum_{\lambda_s, \lambda_t} \langle JMLS|JM\lambda_s\lambda_t\rangle \sqrt{\frac{4\pi}{\rho_s}} \langle JM\lambda_s\lambda_t|\mathcal{M}|JM\rangle \\ &= \sum_{\lambda_s, \lambda_t} \langle JMLS|JM\lambda_s\lambda_t\rangle \frac{N_J}{\sqrt{2J+1}} f_{\lambda_s, \lambda_t}^J \\ &= N_J \sum_{\lambda_s, \lambda_t} \frac{\sqrt{2L+1}}{2J+1} (L0\ S(\lambda_s - \lambda_t)|J(\lambda_s - \lambda_t))(s\lambda_s\ t(-\lambda_t)|S(\lambda_s - \lambda_t)) f_{\lambda_s\lambda_t}^J. \end{aligned}$$

2.3.4. Symmetry Relations. Reactions involving strong or electroweak interactions conserve parity. Parity reverses the direction of \vec{r} and \vec{p} while the angular momentum remains unchanged. Applying the parity transformation on a single particle state one obtains

$$(57) \quad P|\vec{p}, jm\rangle = \eta|\varphi + \pi, \pi - \vartheta, p, jm\rangle$$

in canonical basis and

$$(58) \quad P|\vec{p}, j\lambda\rangle = \eta e^{-i\pi j} |\varphi + \pi, \pi - \vartheta, |\vec{p}|, j - \lambda\rangle$$

in helicity basis with η being the intrinsic parity (± 1) of the particle. For the two-particle states the parity transformation leads to the following relations

$$(59) \quad P|JMls\rangle = \eta_1 \eta_2 (-1)^l |JMls\rangle$$

for the canonical and

$$(60) \quad |JM\lambda_1\lambda_2\rangle = \sum_{l,s} \sqrt{\frac{2l+1}{2J+1}} (l0\ s\lambda|JM)(s_1\lambda_1\ s_2(-\lambda_2)|s\lambda)|JMls\rangle$$

$$(61) \quad P|JM\lambda_1\lambda_2\rangle = \eta_1 \eta_2 (-1)^{J+s_1+s_2} |JMls\rangle$$

for the helicity basis with η_1 , η_2 and η being the intrinsic parities of the two daughters and the decaying particle respectively. This can be used to derive relations for the helicity amplitudes. If parity conservation holds then

$$(62) \quad F_{\lambda_1\lambda_2}^J = \eta \eta_1 \eta_2 (-1)^{J+s_1+s_2} F_{(-\lambda_1)(-\lambda_2)}^J$$

In the special case, that both particles are identical one obtains

$$(63) \quad F_{\lambda_1\lambda_2}^J \stackrel{1 \equiv 2}{=} \eta (-1)^J F_{\lambda_2\lambda_1}.$$

2.3.5. Examples. In this section several examples are given to illustrate the actual handling of the helicity formalism in the day-to-day business.

Example: $f_2(1270) \rightarrow \pi\pi$. The $f_2(1270)$ is an isoscalar tensor particle which means that the initial state has $I^G(J^{PC}) = 0^+(2^{++})$. The two final state pions have $I^G(J^{PC}) = 1^-(0^{-+})$. The intrinsic parity of the $f_2(1270)$ is even, since $\eta_f = \eta_\pi^2 (-1)^l$ and $l = 2$. The total spin $s = 2s_\pi$ is zero. Starting with the definition of the formalism eq. 50

$$A_{\lambda_1\lambda_2}^{JM} = N_J F_{\lambda_1\lambda_2}^J D_{M\lambda}^{J*}(\varphi, \vartheta)$$

and using $\lambda = \lambda_1 - \lambda_2 = 0$ and $J = 2$ we get

$$(64) \quad A_{00}^{2M}(\varphi, \vartheta) = N_2 F_{00}^2 D_{M0}^{2*}(\varphi, \vartheta)$$

$$N_2 F_{00}^2 = \sqrt{5} \underbrace{(20\ 00|00)}_1 \underbrace{(00\ 00|00)}_1 a_{20} = \sqrt{5} a_{20}$$

$$(65) \quad A_{00}^{2M}(\varphi, \vartheta) = \sqrt{5} a_{20} D_{M0}^{2*}(\varphi, \vartheta).$$

Remember that this is a short-hand writing for a whole matrix of amplitudes

$$(66) \quad A_{00}^2(\varphi, \vartheta) = \sqrt{5}a_{20} \begin{pmatrix} d_{(-2)0}^2(\vartheta)e^{-2i\varphi} \\ d_{(-1)0}^2(\vartheta)e^{-i\varphi} \\ d_{00}^2(\vartheta) \\ d_{10}^2(\vartheta)e^{i\varphi} \\ d_{20}^2(\vartheta)e^{2i\varphi} \end{pmatrix}.$$

The intensity is then derived by the bilinear sum of amplitude and conjugated amplitude, weighted by the spin density matrix

$$(67) \quad I(\vartheta) = \sum_{M, M'} A_{00}^{2M}(\varphi, \vartheta) \rho_{MM'} A_{00}^{2M'*}(\varphi, \vartheta)$$

$$\rho = \frac{1}{5} \begin{pmatrix} 1 & & & & \\ & \dots & & & \\ & & & & 1 \end{pmatrix}.$$

Due to cancellation of $\cos \vartheta$ and $\sin \vartheta$ terms, the final result is very simple, it is just a constant:

$$(68) \quad I(\vartheta) = |a_{20}|^2 \left(\frac{15}{4} \sin^4 \vartheta + 15 \sin^2 \vartheta \cos^2 \vartheta + 5 \left(\frac{3}{2} \cos^2 \vartheta - \frac{1}{2} \right) \right)$$

$$= |a_{20}|^2 = \text{const}$$

Example: $\omega \rightarrow \gamma\pi$. The ω is an isoscalar vector particle which means that the initial state has $I^G(J^{PC}) = 0^-(1^{--})$. The final state pion has $I^G(J^{PC}) = 1^-(0^{-+})$ and the photon has $I^G(J^{PC}) = 0(1^{--})$. One should keep in mind that the real photon has no longitudinal component. The intrinsic parity of the ω is $\eta_\omega = \eta_\pi\eta_\gamma(-1)^l$ and the total spin $s = s_\pi + s_\gamma$ is 1. Starting with the definition of the formalism eq. 50

$$A_{\lambda_1\lambda_2}^{JM} = N_J F_{\lambda_1\lambda_2}^J D_{M\lambda}^{J*}(\varphi, \vartheta)$$

and using $\lambda = \lambda_1 - \lambda_2 = \lambda_\gamma = \lambda_1$ and $J = 1$ we get

$$(69) \quad A_{\lambda_0}^{1M}(\varphi, \vartheta) = N_1 F_{\lambda_0}^1 D_{M\lambda}^{1*}(\varphi, \vartheta)$$

$$N_1 F_{\lambda_0}^1 = \sqrt{3} \underbrace{(10 \ 1\lambda | J\lambda)}_{-\frac{\lambda}{\sqrt{2}}} \underbrace{(1\lambda \ 00 | 1\lambda)}_1 a_{11} = -\lambda \sqrt{\frac{3}{2}} a_{11}$$

$$(70) \quad A_{\lambda_0}^{1M}(\varphi, \vartheta) = -\lambda \sqrt{\frac{3}{2}} a_{11} D_{M\lambda}^{1*}(\varphi, \vartheta).$$

or in matrix representation

$$(71) \quad A_{\lambda_0}^1(\varphi, \vartheta) = -\sqrt{\frac{3}{2}} \begin{pmatrix} -d_{(-1)(-1)}^1(\vartheta)e^{-i\varphi} & 0 & -d_{(-1)1}^1(\vartheta)e^{-i\varphi} \\ -d_{0(-1)}^1(\vartheta) & 0 & -d_{01}^1(\vartheta) \\ -d_{1(-1)}^1(\vartheta)e^{i\varphi} & 0 & -d_{11}^1(\vartheta)e^{i\varphi} \end{pmatrix}$$

leading to the intensity

$$(72) \quad I(\vartheta) = \sum_{M, M', \lambda, \lambda'} A_{\lambda_0}^{1M}(\varphi, \vartheta) \rho_{MM'} A_{\lambda_0}^{1M'*}(\varphi, \vartheta) \delta_{\lambda\lambda'}$$

$$\rho = \frac{1}{3} \begin{pmatrix} 1 & & \\ & 1 & \\ & & 1 \end{pmatrix}$$

which finally collapses again to a constant:

$$(73) \quad I(\vartheta) = \frac{1}{2} |a_{11}|^2 \left(2 \left(\frac{1 - \cos \vartheta}{2} \right)^2 + 2 \left(\frac{1 + \cos \vartheta}{2} \right)^2 + 2 \frac{\sin^2 \vartheta}{2} \right)$$

$$= \frac{1}{2} |a_{11}|^2 (1 + \cos^2 \vartheta + \sin^2 \vartheta) = |a_{11}|^2 = \text{const}$$

Example: $f_{0,2}(\text{any}) \rightarrow \gamma\gamma$. The $f_{0,2}$ is an isoscalar scalar or tensor particle which means that the initial state has $I^G(J^{PC}) = 0^+(0^{++} \text{ or } 2^{++})$. The two final state gammas have $I^G(J^{PC}) = 0(1^{--})$. The intrinsic parity of the $f_2(1270)$ is even, since $\eta_f = \eta_\gamma^2(-1)^l$ and $l = 2$. The total spin $s = 2s_\gamma$ is two and thus $l = 0, 2$ are allowed for the f_0 and $l = 0, 2, 4$ are allowed for the f_2 . In the first case we investigate $J = 0$. Following the definition of the formalism eq. 50

$$A_{\lambda_1\lambda_2}^{JM} = N_J F_{\lambda_1\lambda_2}^J D_{M\lambda}^{J*}(\varphi, \vartheta)$$

and using $\lambda = \lambda_1 - \lambda_2$ we get with $J = 0$

$$(74) \quad A_{\lambda_1\lambda_2}^{00}(\varphi, \vartheta) = N_0 F_{\lambda_1\lambda_2}^0 D_{0\lambda}^{0*}(\varphi, \vartheta)$$

$$N_0 F_{00}^0 = \sum_{l,s} (l0s\lambda|J\lambda)(s_1\lambda_1s_2(-\lambda_2)|s\lambda)a_{ls}$$

$$= \sqrt{1}(0000|00)(1\lambda_11(-\lambda_2)|0\lambda)a_{00}$$

$$+ \sqrt{5}(2020|00)(1\lambda_11(-\lambda_2)|2\lambda)a_{22}$$

$$= \sqrt{\frac{1}{3}}a_{00} + \sqrt{\frac{1}{6}}a_{22}$$

$$(75) \quad A_{\lambda_1\lambda_2}^{00}(\varphi, \vartheta) = \left(\sqrt{\frac{1}{3}}a_{00} + \sqrt{\frac{1}{6}}a_{22} \right) \underbrace{D_{00}^{0*}(\varphi, \vartheta)}_1 = \text{const}$$

In the more complicated case for $J =$ we get

$$(76) \quad A_{\lambda_1 \lambda_2}^{2M}(\varphi, \vartheta) = N_2 F_{\lambda_1 \lambda_2}^0 D_{M\lambda}^{2*}(\varphi, \vartheta)$$

$$(77) \quad \begin{aligned} N_2 F_{\lambda_1 \lambda_2}^2 &= \sum_{l,s} (l0s\lambda|J\lambda)(s_1\lambda_1s_2(-\lambda_2)|s\lambda)a_{ls} \\ &= \sqrt{5}(2000|20)(1\lambda_11(-\lambda_2)|00)a_{20} \\ &\quad + \sqrt{5}(202\lambda|2\lambda)(1\lambda_11(-\lambda_2)|2\lambda)a_{22} \\ &\quad + \sqrt{9}(402\lambda|2\lambda)(1\lambda_11(-\lambda_2)|2\lambda)a_{42} \end{aligned}$$

$$(78) \quad = \sqrt{\frac{1}{3}}a_{00} + \sqrt{\frac{1}{6}}a_{22}$$

$$(79) \quad A_{\lambda_1 \lambda_2}^{00}(\varphi, \vartheta) = \left(\sqrt{\frac{1}{3}}a_{00} + \sqrt{\frac{1}{6}}a_{22} \right) \underbrace{D_{00}^{0*}(\varphi, \vartheta)}_1 \text{ const.}$$

Because of the complexity of this result we limit the discussion now to the case where $J = \lambda = 2$. Then a lot of terms disappear and the amplitude contracts to

$$(80) \quad \begin{aligned} N_2 F_{1(-1)}^2 &= \sum_{l,s} (l0s2|22)(s_11s_21|s2)a_{ls} \\ &= \sqrt{5} \underbrace{(20 \ 22|22)}_{\sqrt{\frac{2}{7}}} \underbrace{(11 \ 11|22)}_1 a_{22} + \sqrt{9} \underbrace{(40 \ 22|22)}_{\frac{1}{3\sqrt{14}}} \underbrace{(11 \ 11|22)}_1 a_{42} \end{aligned}$$

Using the symmetrization because of the two identical particles in the final state one gets a fairly simple angular distribution

$$(81) \quad A^{2M} = N_2 (F_{1(-1)} + F_{(-1)1}) D_{M2}^{2*}(\varphi, \vartheta) \propto D_{M2}^{2*}(\varphi, \vartheta).$$

Example: $\bar{p}p \rightarrow \pi\pi$. The $\bar{p}p(0^{-+})$ has $I^G(J^{PC}) = 1^+(J^{PC})$ with $M = 0, \pm 1$. The two final state pions have $I^G(J^{PC}) = 1^-(0^{-+})$. Following the definition of the formalism eq. 50

$$A_{\lambda_1 \lambda_2}^{JM}(\varphi, \vartheta) = N_J F_{\lambda_1 \lambda_2}^J D_{M\lambda}^{J*}(\varphi, \vartheta)$$

and using $\lambda = \underbrace{\lambda_1}_0 - \underbrace{\lambda_2}_0 = 0$ and $J = l$ we get

$$(82) \quad \begin{aligned} A_{00}^{JM}(\varphi, \vartheta) &= N_J F_{00}^J D_{M0}^{J*}(\varphi, \vartheta) \\ N_J F_{00}^J &= \sum_l \sqrt{2l+1} \underbrace{(l0 \ 00|J0)}_1 \underbrace{(00 \ 00|00)}_1 a_{l0} = \sqrt{2J+1} a_{J0} \end{aligned}$$

$$(83) \quad A_{00}^{JM}(\varphi, \vartheta) = \sqrt{2J+1} a_{J0} D_{M0}^{J*}(\varphi, \vartheta) = \sqrt{2J+1} a_{J0} d_{M0}^J(\vartheta) e^{-iM\varphi}$$

The d -functions are not orthogonal, if φ is not observed ambiguities remain in the amplitude and polarization is needed. to disentangle the waves.

Example: $\bar{p}p \rightarrow \omega\pi^0 \rightarrow \gamma\pi^0\pi^0$. This is a two step process $\bar{p}p \rightarrow \omega\pi^0$ and $\omega \rightarrow \gamma\pi^0$ and illustrates how subsequent decays are handled in the helicity formalism. The $\bar{p}p$ has $I^G(J^{PC}) = 1^+(J^{PC})$. The intermediate ω has $I^G(J^{PC}) = 0^-(1^{--})$, the two pions have $I^G(J^{PC}) = 1^-(0^{-+})$ and the photon has $I^G(J^{PC}) = 0(1^{--})$. The angular momentum between the recoil pion and the $f_2(1270)$ is $L = 2$. Using the result from eq. 70 we obtain

$$\begin{aligned}
(84) \quad A_{\lambda_1\lambda_2}^{JM}(\Omega_1, \Omega_2) &= A_{\lambda_\omega\lambda_\gamma}^{JM}(\Omega_{\omega\pi^0}, \Omega_{\pi^0\gamma}) = A_{\lambda_\gamma 0}^{1\lambda_\omega}(\Omega_{\pi^0\gamma}) A_{\lambda_\omega 0}^{JM}(\Omega_{\omega\pi^0}) \\
&= N_{\omega,1} F_{\lambda_\gamma 0}^1 D_{\lambda_\omega\lambda_\gamma}^{1*}(\Omega_{\pi^0\gamma}) N_{\bar{p}pJ} F_{\lambda_\omega 0}^J D_{M\lambda_\omega}^{J*}(\Omega_{\omega\pi^0}) \\
&= -\lambda_\gamma \sqrt{\frac{3}{2}} D_{\lambda_\omega\lambda_\gamma}^{1*}(\Omega_{\pi^0\gamma}) \\
&\quad \times \left(\sum_l \sqrt{2l+1} (l01\lambda_\omega | J\lambda_\omega) a_{\bar{p}p,l1} D_{M\lambda_\omega}^{J*}(\Omega_{\omega\pi^0}) \right) \\
(85) \quad &= -\lambda_\gamma \sqrt{\frac{3}{2}} D_{\lambda_\omega\lambda_\gamma}^{1*}(\Omega_{\pi^0\gamma}) D_{M\lambda_\omega}^{J*}(\Omega_{\omega\pi^0}) \\
&\quad \times \left(\sum_l \sqrt{2l+1} (l01\lambda_\omega | J\lambda_\omega) a_{\bar{p}p,l1} \right)
\end{aligned}$$

The interesting feature of this amplitude is, that the helicity constant $a_{\omega\pi^0,11}$ factorizes and all helicity amplitudes of the $\bar{p}p$ system can be modified to

$$(86) \quad a'_{\bar{p}p,l1} = a_{\bar{p}p,l1} a_{\omega\pi^0,11}$$

Example: $\bar{p}p \rightarrow f_2(1270)\pi^0 \rightarrow \pi^+\pi^-\pi^0$. This is an two step process $\bar{p}p \rightarrow f_2(1270)\pi^0$ and $f_2(1270) \rightarrow \pi^+\pi^-$. The $\bar{p}p(0^{-+})$ has $I^G(J^{PC}) = 1^-(0^{-+})$. The intermediate $f_2(1270)$ has $I^G(J^{PC}) = 0^+(2^{++})$ and the two pions have $I^G(J^{PC}) = 1^-(0^{-+})$. The angular momentum between the recoil pion and the $f_2(1270)$ is $L = 2$. Starting with the definition of the formalism eq. 50

$$A_{\lambda_1\lambda_2}^{JM} = N_J F_{\lambda_1\lambda_2}^J D_{M\lambda}^{J*}(\varphi, \vartheta)$$

and $\lambda = \lambda_1 - \lambda_2 = 0$, $J_{\bar{p}p} = 0$ and $J_{f_2\pi^0} = 2$ we get The full amplitude is then given as (amplitude tree)

$$\begin{aligned}
(87) \quad A_{\lambda_1\lambda_2}^{JM}(\Omega_1, \Omega_2) &= A_{\lambda_1\lambda_2}^{JM}(\Omega_{f_2\pi^0}, \Omega_{\pi^+\pi^-}) = A_{00}^{00}(\Omega_{f_2\pi^0}) A_{20}^{00}(\Omega_{\pi^+\pi^-}) \\
&= N_{\bar{p}p,0} F_{00}^0 D_{00}^{0*}(\Omega_{f_2\pi^0}) N_{f_2,2} F_{00}^2 D_{00}^{2*}(\Omega_{\pi^+\pi^-}) \\
N_{\bar{p}p,0} F_{00}^0 &= \sqrt{1} \underbrace{(20 \ 20|00)}_{\sqrt{\frac{1}{5}}} \underbrace{(20 \ 00|20)}_1 a_{\bar{p}p,22}
\end{aligned}$$

$$\begin{aligned}
N_{f_2,2} F_{00}^2 &= \sqrt{1} \underbrace{(20 \ 00|20)}_1 \underbrace{(00 \ 00|00)}_1 a_{f_2,20} \\
A_{00}^{00}(\Omega_{f_2\pi^0}) A_{20}^{00}(\Omega_{\pi^+\pi^-}) &= \sqrt{5} a_{\bar{p}p,22} a_{f_2,20} D_{00}^{2*}(\underbrace{\Omega_{\pi^+}}_{=(\varphi,\vartheta)}) \underbrace{D_{00}^{0*}(\Omega_{f_2\pi^0})}_1 \\
(88) \qquad \qquad \qquad &= \sqrt{5} a_{\bar{p}p,22} a_{f_2,20} \left(\frac{3}{2} \cos^2 \vartheta - \frac{1}{2} \right).
\end{aligned}$$

with $\Omega_{xy} = (\varphi, \vartheta)$ being the direction of daughter x in the mother system of xy . The final intensity turn out to be simple again:

$$(89) \qquad \qquad \qquad I(\vartheta) = 5 \left| a_{\bar{p}p,22} a_{f_2,20} \right|^2 \left(\frac{3}{2} \cos^2 \vartheta - \frac{1}{2} \right)$$

2.3.6. The $\bar{p}p$ system.

Proton antiproton at rest. The proton antiproton system at rest is formed by an incident antiproton beam on a hydrogen target. Due to Coulomb scattering the antiproton is decelerated according to Bethe-Bloch's formula until it's energy is small enough to be caught by a hydrogen atom. The protonium atom (proton antiproton atomic bound state) is formed at very high n and l of about 30 where it replaces the electron. The system deexcites through slow radiative transitions and through collisions (Auger effect). These processes compete with the Stark mixing of the l levels. Due to the fact, that the protonium atom is much smaller than a usual hydrogen atom it traverses those and feels a very strong electric field which make the levels mix (Day, Snow and Sucher, 1960). The average electric field which is seen by the protonium atom varies with the density of hydrogen atoms and thus depends on the target density. Since in S-wave orbits a annihilation is very probable high density targets (like in liquid hydrogen) have a dominant S-wave yield. In low density targets (like in gaseous hydrogen) more P-wave is present [6]. The advantages of this initial system are manifold

- J^{PC} varies with the target density,
- isospin varies with n (deuterium) or p (hydrogen) targets,
- atomic (incoherent) initial states enable unambiguous partial wave decomposition.

But there are also some disadvantages like

- limited phase space and a very small kaon yield.

The $\bar{p}p$ system has an invariant mass of $m_{\bar{p}p} \approx 1877 \text{ MeV}/c^2$. Since a recoil particle is needed to ensure energy and momentum balance investigations are only possible up to a mass of $m_{Meson} \approx 1700 \text{ MeV}/c^2$. If due to quantum number requirements another (heavier) recoil particle is required, the phase space limits are even more severe.

In principle the same kind of physics could be investigated using an \bar{n} beam. This has been done by the Obelix collaboration. Since the \bar{n} as the n is neutral, there is now deceleration in material and no neutronium atom. But one can do annihilations in flight which is discussed in the next subsection. This is not true for annihilation of an antiproton on the neutron of a deuteron, since the deuteron and the antiproton also form a bound atomic system.

The annihilation - being a strong process - conserves all quantum numbers from the atomic state. The most important ones are

- $G = (-1)^{I+L+S}$,
- $P = (-1)^{L+1}$,
- $C = (-1)^{L+S}$ and $CP = (-1)^{S+1}$.

The isospin of a $\bar{p}p$ system can be either 0 or 1. Therefore in the isospin space the protonium system mixes with the neutronium and the wave functions for the initial state are

- $\frac{1}{\sqrt{2}}(|\bar{p}p\rangle + |\bar{n}n\rangle)$ has $I=0$,
- $\frac{1}{\sqrt{2}}(|\bar{p}p\rangle - |\bar{n}n\rangle)$ has $I=1, I_3=0$ and
- $|\bar{p}n\rangle$ has $I=1, I_3=+1$.

Usually only S - and P -waves are taken into account. In liquid hydrogen the S -wave is dominant with a yield of more than 90%. In gaseous hydrogen at NTP the ratio between S - and P -wave is around 1. In low pressure targets the P -wave yield may be as much as 90% [7]. Since the atomic system lives quite long compared to the strong interaction it rotates many times until it finally annihilates. Therefore the helicity of the initial antiproton is of no use. The population density is just equally distributed for all helicities or in other terms for all values of the magnetic quantum number.

Proton antiproton in flight. With higher antiproton momenta a higher center of mass energy can be reached and thus more massive mesons can be produced. In addition there is the possibility to create resonances without recoil particles which makes the analysis much easier and less ambiguous, although not all quantum numbers are accessible (only fermion anti-fermion quantum numbers remain to be producible). The annihilation of $\bar{p}p$ at higher incident momenta is completely different to the situation at rest. There are no more atomic levels. As soon as the antiproton is too fast to be captured one deals with a scattering process. The number of partial waves rise with increasing momenta and detailed investigations show that the maximum needed angular momentum is $l \approx p_{cms}/200 \text{ MeV}/c^2$ which is almost compatible with statistical models. This leads to a huge amount of waves where most of them are allowed to interfere. But there are some constraints which limit the amplitudes to be considered.

Since we have a fermion anti-fermion system helicity conservation reduces the initial helicities to 0 or 1 with the symmetry relation $H_{\nu_1\nu_2}^J = \eta_J(-1)^J H_{-\nu_2(\nu_1)}^J$ with helicities $\nu_{1,2}$ for the proton and the antiproton respectively and total angular momentum J . From C and CP invariance one gets in addition $H_{11} = 0$ if $L + S + J$ is odd and $H_{-1(1)} = 0$ if $S = 0$ and/or $J = 0$. Since C and CP are conserved interference is only possible in between waves where C and CP are equal. This decouples singlet and triplet states as well as it decouples even from odd L . In total four incoherent sets of amplitudes remain. The final state poses additional constraints so that many amplitudes vanish due to other conservation laws. Nevertheless the number of parameters for a partial wave analysis is still very high and can easily exceed 100. Therefore it might be possible that in many cases the amplitudes have to be simplified with the cost of giving informations and constraints away.

If there is a formation process with two particles in the final state a full featured amplitude is usually applicable and produces unambiguous results [8]. But if there are three and more particles involved and the number of resonances is large it is necessary to reduce the complexity of the fit by integrating out the production process and concentrating on the final state. Many constraints from the initial state are lost that way but the number of parameters can be handled easier. The main caveat is the handling of coherence. For two fully coherent amplitudes the intensity looks like $I = |A + ei\phi B|^2 = |A|^2 + |B|^2 + 2(\Re[AB^*] \sin \varphi + \Im[AB^*] \cos \varphi)$. If there is no coherence it is $I = |A|^2 + |B|^2$. In the case of a mixture of coherent and incoherent terms an effective coherence is needed which can be defined like $I = |A|^2 + |B|^2 + c(\Re[AB^*] \sin \varphi + \Im[AB^*] \cos \varphi)$ with $c = -2, \dots, 2$. This technique leaves in the possibility to check whether or not coherence between two amplitudes is needed at all [9].

Other anti-nucleon nucleon systems. There are actually two other techniques which have been used apart from $\bar{p}p$ annihilation. One is the $\bar{n}n$ annihilation by Obelix. This reaction cannot occur from an atomic state, but as an in flight reaction. This is done by using a antiproton beam to produce antineutrons in the reaction $\bar{p}p \rightarrow \bar{n}n$. This produces antineutrons in a broad energy range. They annihilate on a deuterium target and the neutral events are selected with zero net charge in the final event. The quantum numbers can be applied as in the $\bar{p}p$ case in flight. The usual energy range does not exceed 300 MeV/c so angular momenta up to D-wave are sufficient to fit the data. The other technique is to use a antiproton beam on a deuterium target and by selecting the net charge of the event a selection of $\bar{p}p$ and $\bar{p}n$ reactions is possible. In addition information comes from the spectating nucleon, either a proton or a neutron. The antiproton is in an atomic orbit of the deuteron before annihilation, but the levels are somewhat different (due to the different reduced mass of the system) and the base system for the waves is the center of mass of the deuteron, and not the individual nucleon which takes part of the annihilation. In addition, there is Fermi motion of the nucleons inside the deuteron. To select the initial angular momentum of the whole system the breakup momentum of the spectator is used. If the momentum is small ($p_{spec} < 100$ MeV/c) the process is

dominated by S-wave. Due to the momentum range all phase space boundaries (like in Dalitz plots) remain fuzzy.

2.4. Moments Analysis. – The basic idea of this approach is to do a Fourier decomposition of the final state. This is done for each bin of invariant masses of the exclusive final state system. This method is explained best by using an example. For an unpolarized target and without measuring the recoil polarization of the neutron in a charge exchange reaction of the type

$$(90) \quad \pi^- + p \rightarrow M^0 + n \quad \text{and} \quad M^0 \rightarrow a + b$$

the differential cross section can be written [10] as

$$(91) \quad I(t, M, \vartheta, \varphi) = \frac{\partial^4 \sigma}{\partial t \partial M \partial \cos \vartheta \partial \varphi} = \frac{1}{2} \sum_{\lambda_p, \lambda_n} |H_{\lambda_p \lambda_n}(t, M, \vartheta, \varphi)|^2$$

where t is the momentum transfer between the incident π^- and the M^0 system, M is the M^0 invariant mass, λ_p, λ_n are the proton and neutron helicities and ϑ, φ are the polar and azimuthal angles of either particle a , or b in the Gottfried-Jackson frame ⁽¹⁾. The full helicity amplitude $H_{\lambda_p \lambda_n}(t, M, \vartheta, \varphi)$ which is the sum of the terms corresponding to all possible intermediate spin j and helicity m states of M^0 is given by

$$(92) \quad \sqrt{4\pi} H_{\lambda_p \lambda_n}(t, M, \vartheta, \varphi) = \sum_{j=0}^{\infty} \sum_{m=-j}^j \sqrt{2j+1} H_{\lambda_p \lambda_n, m}^j d_{m0}^j(\vartheta) e^{im\varphi}.$$

Inserting eq. 92 in eq. 91 one gets

$$(93) \quad \begin{aligned} 4\pi I(\vartheta, \varphi) &= \frac{1}{2} \sum_{\lambda_p, \lambda_n} \sum_{j_2, m_2} \sum_{j_1, m_1} \sqrt{2j_1+1} \sqrt{2j_2+1} e^{i(m_1 - m_2)\varphi} \\ &= \times H_{\lambda_p, \lambda_n, m_1}^{j_1*} H_{\lambda_p, \lambda_n, m_2}^{j_2} d_{m_1 0}^{j_1}(\vartheta) d_{m_2 0}^{j_2}(\vartheta) \end{aligned}$$

The helicity products of relation eq. 93 can be expressed in terms of the density matrix

$$(94) \quad \rho_{m_1 m_2}^{j_1 j_2} = \frac{1}{2N} \sum_{\lambda_p, \lambda_n} H_{\lambda_p, \lambda_n, m_1}^{j_1*} H_{\lambda_p, \lambda_n, m_2}^{j_2}$$

where $N = \frac{\partial^2 \sigma}{\partial t \partial M}$. Therefore eq. 93 can be rewritten as

$$(95) I(\vartheta, \varphi) = \frac{N}{4\pi} \sum_{j_2, m_2, j_1, m_1} \sqrt{2j_1+1} \sqrt{2j_2+1} \rho_{m_1 m_2}^{j_1 j_2} d_{m_1 0}^{j_1}(\vartheta) d_{m_2 0}^{j_2}(\vartheta) e^{i(m_1 - m_2)\varphi}$$

⁽¹⁾ The Gottfried-Jackson frame is the M^0 frame rotated so that its z -axis is parallel to the incident π^- direction.

and its integral gives the trace equality

$$(96) \quad \sum_{j,m} \rho_{mm}^{jj} = 1.$$

As the strong interaction conserves parity, for the process $1 + 2 \rightarrow 3 + 4$, the helicity amplitudes satisfy the relation

$$(97) \quad H_{\lambda_3, \lambda_4, \lambda_1, \lambda_2} = \eta(-1)^k H_{-\lambda_3, -\lambda_4, -\lambda_1, -\lambda_2}$$

whre η is the intrinsic parity product of the particles 1, 2, 3 and 4 and $k = \sum_i (s_i + \lambda_i)$ is the sum of their spins and helicities. Combining eq. 97 and eq. 94 one obtains

$$(98) \quad \rho_{m_1 m_2}^{j_1 j_2} = (-1)^{m_1 + m_2} \rho_{(-m_1)(-m_2)}^{j_1 j_2}.$$

In any reference frame where the z -axis is in the production plane, the most general angular distribution of the M^0 system can be written, according to parity conservation, as a sum of the real parts $\Re[Y_l^m]$ of the spherical harmonic moments. For simplicity we will write Y_l^m instead of $\Re[Y_l^m]$

$$(99) \quad I(t, M, \vartheta, \varphi) = N \sum_{l=0}^{\infty} \sum_{m=-l}^l \langle Y_l^m \rangle Y_l^m(\vartheta, \varphi)$$

where $\langle Y_l^m \rangle$ are the normalized moments. In particular $\langle Y_0^0 \rangle = \frac{1}{4\pi}$ and $Y_0^0 = 1$.

Using standard relations amongst rotation matrix products, the $\langle Y_l^m \rangle$ coefficients can be expressed as a sum of the real parts of the elements $\rho_{m_1 m_2}^{j_1 j_2}$

$$(100) \quad \langle Y_l^m \rangle = \frac{1}{4\pi} \sum_{j_2, m_2, j_1, m_1} (-1)^{m-m_2} \sqrt{(2l+1) \frac{2j_1+1}{2j_2+1}} (lm \ j_1(-m_1) | j_2(-m_2)) (l0 \ j_1 0 | j_2 0) \Re[\rho_{m_1 m_2}^{j_1 j_2}].$$

Together with eq. 94 it is easy to see, that the $\langle Y_l^m \rangle$ can be expressed as bilinear forms of helicity amplitudes.

Including the factor N in the coefficients $\langle Y_l^m \rangle$, one obtains a new set of coefficients t_l^m which depend on the momentum transfer t and the mass M of the M^0 system. The angular distribution of the produced events can then be written as

$$(101) \quad I_{prod}(t, M, \vartheta, \varphi) = \sum_{l=0}^{\infty} \sum_{m=0}^l t_l^m Y_l^m(\vartheta, \varphi)$$

This set of coefficients is obtained by fitting eq. 101. To obtain the different waves, which contribute to a specific moment the relation eq. 100 has to be inverted. Since this is a

non-linear system of equation there are several solutions and it has to be ensured in the analysis process, that the different solutions show the same physical behavior. Otherwise the data will not be conclusive.

An example with only S - and P -wave may serve to illustrate the details. For $l \leq 1$ there are only two components

$$(102) \quad f(\vartheta) = \langle S \rangle P_0(\cos \vartheta) + 3\langle P \rangle P_1(\cos \vartheta) = \langle S \rangle + 3\langle P \rangle \cos \vartheta$$

3. – Dynamical Amplitudes

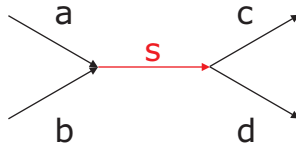


Fig. 6. – s-Channel scattering.

3.1. S -Matrix. – Consider a two-body scattering of the type $ab \rightarrow cd$ (like in fig. 6). The differential cross section is given in terms of the invariant amplitude \mathcal{M} and the ‘scattering amplitude’ f through

$$(103) \quad \frac{d\sigma_{fi}}{d\Omega} = \frac{1}{(8\pi)^2 s} \left(\frac{q_f}{q_i} \right) |\mathcal{M}_{fi}|^2 = |f_{fi}(\Omega)|^2$$

where ‘ i ’ and ‘ f ’ stand for the initial and final states; $\Omega = (\theta, \phi)$ denotes the usual spherical coordinate system; and $s = m^2$ is the square of the center-of-mass (CM) energy. The $q_i(q_f)$ is the breakup momentum in the initial(final) system. [The observed cross section is in reality the average of the initial spin states and the sum over all final spin states— this is suppressed here for simplicity.] The scattering amplitude can be expanded in terms of the partial-wave amplitudes

$$(104) \quad f_{fi}(\Omega) = \frac{1}{q_i} \sum_J (2J+1) T_{fi}^J(s) D_{\lambda\mu}^{J*}(\phi, \theta, 0)$$

where $\lambda = \lambda_a - \lambda_b$ and $\mu = \lambda_c - \lambda_d$ in terms of the helicities of the particles involved in the scattering $ab \rightarrow cd$. Note that this ‘scattering amplitude’ is a factor of two bigger than that with a more common definition (for example, see Section 5.1, Chung [11]). One may in addition note that the argument of the D -function is frequently given as $(\phi, \theta, -\phi)$ (see Jacob and Wick [2] and Martin and Spearman [12]). Integrating the differential cross section over the angles, one finds, for the cross section in the partial wave J ,

$$(105) \quad \sigma_{fi}^J = \left(\frac{4\pi}{q_i^2} \right) (2J+1) |T_{fi}^J(s)|^2$$

Note that T^J has no unit; the unit for the cross section is being carried by q_i^2 . It is necessary to define more precisely the initial and the final states

$$(106) \quad |i\rangle = |ab, JM\lambda_a\lambda_b\rangle$$

$$(107) \quad |f\rangle = |cd, JM\lambda_c\lambda_d\rangle$$

where M is the z-component of total spin J in a coordinate system fixed in the overall CM frame and the notations $\{ab\}$ and $\{cd\}$ designate additional informations needed to fully specify the initial and the final states. Because of conservation of angular momentum, an initial state in $|JM\rangle$ remains the same in the scattering process. Note the normalization (see Section 4.2, Chung [11])

$$(108) \quad \langle f|i\rangle = \delta_{ij}$$

In the remainder of this section and in subsequent sections, it is to be understood that the ket states mentioned always refer to those of eq. 107. In particular, explicit references to the total angular momentum J will be suppressed. Note that, with this convention, one has eliminated the necessity of specifying continuum variables such as angles and momenta.

In general, the amplitude that an initial state $|i\rangle$ will be found in the final state $|f\rangle$ is

$$(109) \quad S_{fi} = \langle f|S|i\rangle$$

where S is called the scattering operator. One may remove the probability that the initial and final states do not interact at all, by defining the transition operator T through

$$(110) \quad S = I + 2i T$$

where I is the identity operator. The factors 2 and i have been introduced for convenience. From conservation of probability, one deduces that the scattering operator S is unitary, i.e.

$$(111) \quad S S^\dagger = S^\dagger S = I$$

3.2. *T*-Matrix. –

3.2.1. Harmonic Oscillator and the Lorentz-Function.

Harmonic Oscillator. As an academic example toward the discussion about the properties of the T -matrix and how to obtain a reasonable parametrization we go back to the classical harmonic oscillator. from the Lagrange function

$$(112) \quad L = \frac{m}{2} \dot{x}^2 - \frac{kx^2}{2}$$

and the Lagrange equations

$$(113) \quad \frac{d}{dt} \frac{\partial L}{\partial \dot{x}_i} = \frac{\partial L}{\partial x_i}$$

one can derive the equation of motion, which is in this case the well known formula

$$(114) \quad \ddot{x} + \omega_0^2 x = 0$$

If the oscillator is damped and periodic forces are applied to the damped harmonic system like

$$(115) \quad \ddot{x} + 2\lambda\dot{x} + \omega_0^2 x = \frac{f}{m} \cos \omega_R t = \frac{f}{m} \Re [e^{i\omega_R t}]$$

leads to the time averaged intensity (over a half period) in the proximity of the resonance

$$(116) \quad I(\omega_R) = \frac{f^2}{4m} \frac{\lambda}{(\omega_R - \omega_0)^2 + \lambda^2}.$$

This function is called Lorentz function and has the phase δ with

$$(117) \quad \tan \delta = \frac{2\lambda\omega_R}{\omega_0^2 - \omega_R^2}.$$

and has a maximum for $\omega_R = \omega_0$ with a value of $I_0 = I(\omega_0) = \frac{f^2}{4m}$.

Primer in Scattering Theory. In scattering theory a line shape of a resonance is obtained by solving the Schrödinger equation. For two spinless particles with masses m_1 and m_2 the interaction can be described by a spherical potential with $V(\vec{r}) = V(|\vec{r}|) = V(r)$. The Schrödinger equation is defined like

$$(118) \quad -\frac{\hbar^2}{2\mu^2} \nabla^2 \Psi + V(r)\Psi = E\Psi$$

with the reduced mass $\mu = \frac{m_1 m_2}{m_1 + m_2}$. The incoming particle is assumed to be a free particle, represented by an incoming wave. If the particle moves in z we get

$$(119) \quad \Psi_i = e^{ikz} \text{ with } \vec{k} = \frac{\vec{p}}{\hbar}.$$

The incoming wave can be expanded in partial waves

$$(120) \quad \Psi_i = \sum_{l=0}^{\infty} U_l(r) P_l(\cos \theta)$$

where U_l are the solutions of the free ($V = 0$) radial equation.

$$(121) \quad \frac{d^2}{dr^2} U_l(r) + \left(k^2 - \frac{l(l+1)}{r} \right) U_l(r) = 0.$$

The asymptotic behaviors of the wave for $kr \rightarrow \infty$ is

$$(122) \quad \Psi_{i,kr \rightarrow \infty} = e^{ikz} = \sum_{l=0}^{\infty} \frac{i^l (2l+1)}{2lkr} \left[e^{i \left(kr - \frac{l\pi}{2} \right)} - e^{i \left(kr + \frac{l\pi}{2} \right)} \right].$$

Without interaction we get $\Psi_f = \Psi_i$. Even with interaction the incoming wave remains unchanged, while the phase of the outgoing wave is moved by 2δ and the amplitude is reduced by a factor η . The asymptotic behavior is

$$(123) \quad \Psi_{i,kr \rightarrow \infty} = \sum_{l=0}^{\infty} \frac{i^l (2l+1)}{2lkr} \left[\eta_l e^{2i\delta_l} e^{i \left(kr - \frac{l\pi}{2} \right)} - e^{i \left(kr + \frac{l\pi}{2} \right)} \right].$$

The difference between the incoming and outgoing wave defines the scattering wave.

$$(124) \quad \begin{aligned} \Psi_s &= \Psi_f - \Psi_i \\ &= \frac{1}{k} \sum_{l=0}^{\infty} (2l+1) \frac{\eta_l e^{2i\delta_l} - 1}{2l} P_l(\cos \theta) \frac{e^{ikr}}{r} \end{aligned}$$

$$(125) \quad = \frac{1}{k} \sum_{l=0}^{\infty} (2l+1) T_l P_l(\cos \theta) \frac{e^{ikr}}{r}$$

$$(126) \quad = f(\theta) \frac{e^{ikr}}{r}.$$

Eq. 126 contains two important definitions:

$$(127) \quad T_l = \frac{\eta_l e^{2i\delta_l} - 1}{2l}$$

$$(128) \quad f(\theta) = \frac{1}{k} \sum_{l=0}^{\infty} (2l+1) T_l P_l(\cos \theta)$$

Another important result, is that the total cross section is proportional to the imaginary part of the forward scattering amplitude. This is well known as the optical theorem:

$$(129) \quad \sigma_T = \frac{4\pi}{k} \Im [f(0)]$$

with the scattering amplitude $f(\vartheta)$ defined as

$$\begin{aligned}
 \Psi_S &= f(\vartheta) \frac{e^{ikr}}{r} \\
 (130) \quad f(\vartheta) &= \frac{1}{k} \sum_{l=0}^{\infty} (2l+1) \frac{\eta_l e^{2i\delta_l} - 1}{2i} P_l(\cos \vartheta) \\
 f(\vartheta) &= \frac{1}{k} \sum_{l=0}^{\infty} (2l+1) T^l P_l(\cos \vartheta).
 \end{aligned}$$

Using $\theta = 0 \Rightarrow \cos \theta = 1 \Rightarrow P_l(1) \equiv 1$ we get

$$(131) \quad \sigma_T = \sigma_E + \sigma_I = \frac{4\pi}{k} \sum_{l=0}^{\infty} (2l+1) \Im [T_l].$$

To derive explicit forms for σ_E and σ_I we now investigate the imaginary part of the T -matrix:

$$\begin{aligned}
 (132) \quad \Im [T_l] &= \Im \left[\frac{\eta_l e^{2i\delta_l} - 1}{2i} \right] \\
 &= \Im \left[\frac{-\eta_l e^{2i\delta_l} + i}{2} \right] \\
 &= \frac{1}{2} \Im [\eta_l \sin(2\delta_l) + i(-\eta_l \cos 2\delta_l + 1)] \\
 &= \frac{1}{4} (-\eta_l \cos 2\delta_l + 2) \\
 &= \frac{1}{4} (-\eta_l \cos 2\delta_l + 1 + \eta_l^2 + 1 - \eta_l^2) \\
 (133) \quad &= \frac{1}{4} \left(\left| \frac{\eta_l e^{2i\delta_l} - 1}{i} \right|^2 + (1 - \eta_l^2) \right).
 \end{aligned}$$

From this we get for the elastic cross section (using eq. 131)

$$\begin{aligned}
 \sigma_E &= \frac{4\pi}{k} \sum_{l=0}^{\infty} (2l+1) \left| \frac{\eta_l e^{2i\delta_l} - 1}{2i} \right|^2 \\
 (134) \quad &= \frac{4\pi}{k} \sum_{l=0}^{\infty} (2l+1) |T_l|^2
 \end{aligned}$$

and correspondingly for the inelastic cross section

$$(135) \quad \sigma_I = \frac{\pi}{k^2} \sum_{l=0}^{\infty} (2l+1) (1 - \eta_l^2).$$

For the fully elastic case the T -matrix reduces to the simple form

$$\begin{aligned}
 (136) \quad T_l &= \frac{e^{2i\delta_l} - 1}{2i} = e^{i\delta_l} \sin(\delta_l) \\
 &= \frac{\sin(\delta_l)}{e^{i\delta_l}} = \frac{\sin \delta_l}{\cos \delta_l - i \sin \delta_l} \\
 (137) \quad &= \frac{1}{\cot \delta_l - i}.
 \end{aligned}$$

3.2.2. Simple and Relativistic Breit-Wigner Function.

Decay of Unstable States. We assume a state which can be either a resonance in scattering theory or a metastable state in an atom. The wave function of the non-stationary state of frequency $\omega_R = \frac{E_R}{\hbar}$ and lifetime $= \frac{\hbar}{\Gamma}$ can be written as

$$\begin{aligned}
 (138) \quad \psi(t) &= \Psi_0 e^{-\omega_R t} e^{-\frac{t}{2\tau}} \\
 &= \Psi_0 e^{-\omega_R t} e^{-\frac{\Gamma}{2} t}.
 \end{aligned}$$

Ψ as a function of the frequency is derived from a Fourier transformation

$$\begin{aligned}
 (139) \quad \Psi(\omega) &= \frac{1}{\sqrt{2\pi}} \int_{-\infty}^{\infty} \psi(t) e^{i\omega t} dt \\
 &= \frac{\Psi_0}{\sqrt{2\pi}} \int_{-\infty}^{\infty} e^{i\left(\omega - \omega_R + i\frac{\Gamma}{2}\right)t} dt \\
 &= \frac{\Psi_0}{\omega - \omega_R - i\frac{\Gamma}{2}} \left[\frac{1}{\sqrt{2\pi}} e^{i\left(\omega - \omega_R + i\frac{\Gamma}{2}\right)t} \right]_{-\infty}^{\infty} \\
 (140) \quad &= \frac{\kappa}{(E_R - E) - i\frac{\Gamma}{2}}
 \end{aligned}$$

where the constant κ is determined by the normalization of the wave function. To get the connection to scattering theory, we determine κ with the formulae of the previous paragraphs. In the case of elastic scattering (the resonance decays only in one elastic channel $m_1 + m_2 \rightarrow R \rightarrow m_1 + m_2$) the maximum cross section for a given l is (see eq. 134)

$$(141) \quad (\sigma_E^l)_{\max} = \frac{4\pi}{k} (2l + 1).$$

On the other hand the elastic cross section is proportional to the absolute square of the wave function $\sigma_E \propto \Psi\Psi^*$. Since $(\Psi\Psi^*)_{\max} = \frac{4\kappa^2}{\Gamma^2}$, we get the Breit-Wigner formula with $\kappa = \frac{\Gamma}{2}$

$$(142) \quad \Psi(E) = \frac{\frac{\Gamma}{2}}{(E_R - E) - i\frac{\Gamma}{2}}.$$

The elastic cross section is then

$$(143) \quad \sigma_E^l = \frac{4\pi}{k}(2l+1) \frac{\frac{\Gamma^2}{4}}{(E_R - E)^2 + \frac{\Gamma^2}{4}}.$$

Breit-Wigner from Phase Movement. In the case of elastic scattering of spinless particles via a resonance of spin $J = l$ we start with $T = \frac{1}{\cot \delta - i}$. In the proximity of the resonance it is well known that $\delta \approx \frac{\pi}{2} \Rightarrow \cot \delta \approx 0$ and $E_R = E(\delta = \frac{\pi}{2})$. We expand $\cot \delta$ and get

$$(144) \quad \cot \delta(E) = \cot \delta(E_R) + (E - E_R) \left[\frac{d}{dE} \cot \delta(E) \right]_{E=E_R}$$

$$(145) \quad = 0 + (E - E_R) \left(-\frac{\Gamma}{2} \right)$$

where $\frac{\Gamma}{2}$ was defined as the first derivative of the $\cot \delta$. From this we obtain

$$(146) \quad T = \frac{1}{\cot \delta - i} = \frac{\frac{\Gamma}{2}}{(E_R - E) - i\frac{\Gamma}{2}}$$

which is only valid for $|E - E_R| \approx \Gamma \ll E_R$.

Breit-Wigner from Field Theory. A different way is to start from field theory and to derive a dynamic function, e.g. a Breit-Wigner, from a propagator approach. Let's

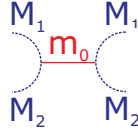


Fig. 7. – Resonant scattering. A pair of mesons undergoes a resonant scattering and appears again in the final state.

suppose we start with a process like the one in fig. 7. The transition amplitude, respective the T -matrix can be written like

$$(147) \quad T = V_{12} \frac{1}{E_0 - E} V_{12}$$

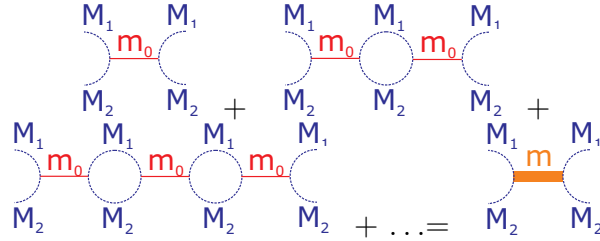


Fig. 8. – T -Matrix from perturbation.

where the transition is constructed from a propagator and the two couplings at the vertices. But that is not the end of the story since more loops can open up like

$$(148) \quad T = V_{12} \frac{1}{E_0 - E} b \frac{1}{E_0 - E} V_{12} = \frac{V_{12} b V_{12}}{(E_0 - E)^2}$$

and finally the transition amplitude is constructed from an infinite series of propagations (see fig. 8) where the strength gets smaller by the factor b for each additional loop:

$$(149) \quad T = V_{12} \frac{1}{E_0 - E} V_{12} + \frac{V_{12} b V_{12}}{(E_0 - E)^2} + \frac{V_{12} b^2 V_{12}}{(E_0 - E)^3} + \dots$$

This can be written as a geometric series

$$(150) \quad \begin{aligned} T &= \frac{V_{12} V_{12}}{E_0 - E} \left(1 + \frac{b}{E_0 - E} + \frac{b^2}{(E_0 - E)^2} + \dots \right) \\ &= \frac{V_{12} V_{12}}{E_0 - E} \left(\frac{1}{1 - \frac{b}{E_0 - E}} \right) \\ &= \frac{V_{12} V_{12}}{E_0 - E - b}. \end{aligned}$$

Since b is complex we get

$$(151) \quad \begin{aligned} T &= \frac{V_{12} V_{12}}{E_0 - \Re[b] - E - i\Im[b]} \\ &= \frac{V_{12} V_{12}}{E_R - E - i\Im[b]}. \end{aligned}$$

Relativistic Breit-Wigner. All discussions so far were based on non-relativistic forms. Since most reactions in meson spectroscopy involve relativistic particles a relativistic formulae is mandatory for any serious data analysis. Without prove and omitting some details here is sketch toward a covariant description.

Starting with the optical theorem in a slightly different form

$$(152) \quad \Im [T(s, 0)] = \frac{q}{4\pi} \frac{\sqrt{s}}{2} \sigma_T$$

we derive

$$(153) \quad T_l(s) = \frac{\sqrt{s}}{2} \frac{1}{\cot \delta - i}$$

with the inverse T -matrix (dropping l for ease of writing)

$$(154) \quad T^{-1}(s) = \frac{q}{\sqrt{s}} (\cot \delta - i) = k(s) - i \frac{2q}{\sqrt{s}}.$$

The matrix $k(s)$ will later be introduced as K -matrix (see sec. **3**3.1). $k(s)$ can be any real valued function. $T(s)$ has a ‘peak’, e.g. a resonance, if $k(s) = 0$. The simplest covariant function with this property is $k(s) = \frac{s_r - s}{\gamma}$ from which we obtain the relativistic Breit-Wigner function

$$(155) \quad T(s) = \frac{\gamma}{s_r - s - i \frac{2q\gamma}{\sqrt{s}}}.$$

32.3. Centrifugal Barrier. From the covariant description of the decay amplitudes, one can show that the mass dependent width of the resonances are proportional to q^{2l+1} . This is known as the centrifugal barrier. Taking out the phase space factor $\rho = \sqrt{2q/m}$ the remaining width is still proportional to q^{2l} . This is only valid for low energies (where they are very important) and a more general formalism is needed to accommodate for the properties of a scattered wave far away from thresholds where the q^{2l+1} rule is invalid.

For fixed-channel orbital angular momentum L these effects are correlated in a simple way with the semi-classical impact parameter

$$(156) \quad b = [L(L+1)]^{\frac{1}{2}} / q$$

where q is the channel wave number. When b is large (q small), cross sections and partial decay widths are relatively suppressed. In any two-body resonance decay channel n with orbital momentum $L \neq 0$, the form of the radial wave function will be determined dominantly by the repulsive centrifugal barrier and the channel wave number q_n for a particle separation r greater than a certain ‘interaction radius’ (R). The approximate wave equation which holds outside R is

$$(157) \quad \frac{\partial^2}{\partial \rho^2} U_l^n \rho \simeq \left(\frac{b_n^2}{r^2} - 1 \right) U_l^n \rho$$

where $\rho = q_n r$ and $b_n = [L(L+1)]^{1/2}/q_n$ is again the impact parameter. The solution for eq. 157 is proportional to the spherical Hankel function

$$(158) \quad U_l^n \rho \stackrel{r \gg R}{\simeq} i C_n \rho h_l^{(1)}(\rho) \sim C_n e^{i\left(\rho - \frac{1}{2}L\pi\right)}$$

where C_n is a constant. Consider the situation if R is very small compared to b : for $r < b$, the radial probability density grows rapidly with decreasing r . The reason is that the outgoing wave is reflected inward by the centrifugal barrier. At $r = R$, the radial probability density is

$$(159) \quad [T_l^n(R/b)]^{-1} \equiv \rho^2 |h_l^{(1)}(\rho)|^2.$$

For a decay, we are interested on the lifetime which is involved with the centrifugal barrier. In general we obtain a reduced width γ_n . In addition the factor q_n/m is taken out of the physical partial width Γ_n so that

$$(160) \quad \Gamma_n = \gamma_n \frac{q_n}{m} T_l^n(R/b_n)$$

$$(161) \quad \Gamma_n(q_n) = \Gamma_n^0 \frac{\frac{q_n}{m} T_l^n(R/b_n)}{\frac{q_n^0}{m} T_l^n(R/b_n^0)}$$

where m is the mass of the decaying particle and q_n/m accounts for the two-body phase space. How do they actually look like. The spherical Hankel functions are defined in terms of ordinary Hankel functions of half-odd-integer order:

$$(162) \quad \begin{aligned} j_l(x) &\equiv \frac{\pi}{2x} J_{l+\frac{1}{2}}(x) \\ n_l(x) &\equiv \frac{\pi}{2x} N_{l+\frac{1}{2}}(x) \\ h_l^{(1,2)}(x) &\equiv \frac{\pi}{2x} \left[J_{l+\frac{1}{2}}(x) \pm N_{l+\frac{1}{2}}(x) \right] \end{aligned}$$

For real values of x , $h_l^{(1)}(x) = [h_l^{(2)}(x)]^*$. The explicit forms of the first three spherical Hankel functions are

$$(163) \quad h_0^{(1)}(x) = \frac{e^{ix}}{ix}$$

$$(164) \quad h_1^{(1)}(x) = \frac{-e^{ix} \left(1 + \frac{i}{x}\right)}{x}$$

$$(165) \quad h_2^{(1)}(x) = i \frac{e^{ix} \left(1 + \frac{3i}{x} - \frac{3}{x^2}\right)}{x}$$

The asymptotic behavior of the spherical Hankel functions for small arguments $x \ll l$ may be inferred from the forms of the spherical Bessel functions

$$(166) \quad \begin{aligned} j_l(x) &\rightarrow \frac{x^l}{(2l+1)!!} \\ n_l(x) &\rightarrow \frac{-(2l-1)!!}{x^{l+1}} \end{aligned}$$

where the double factorial is defined as $x!! = x(x-2)(x-4)\dots$. The eq. 163-165 then translate into

$$(167) \quad \begin{aligned} F_l(q) &= F_l(x = \frac{q}{q_{scale}}) = \sqrt{\frac{|h_l^{(1)}(x)|^2}{|h_l^{(1)}(x=1)|^2}} \\ F_l(q) &\stackrel{q \rightarrow q_{scale}}{=} 1 \\ F_l(q) &\stackrel{q \rightarrow 0}{=} q^l. \end{aligned}$$

And finally we obtain the damping functions for $l = 0$ to 3.

$$(168) \quad \begin{aligned} F_0(x) &= 1 \\ F_1(x) &= \sqrt{\frac{x}{x+1}} \\ F_2(x) &= \sqrt{\frac{13x^2}{(x-3)^2 + 9x}} \\ F_3(x) &= \sqrt{\frac{277x^3}{x(x-15)^2 + 9(2x-5)^2}} \end{aligned}$$

They are applied to the natural width with the factor B_l^2 which are defined as

$$(169) \quad B_l(q, q_R) = \frac{F_l(q)}{F_l(q_R)}$$

3.2.4. Required Properties for T . The main requirement is the analyticity of T . An empirical fact is the appearance of singularities, e.g. poles, which are accommodated by allowing a finite number of poles in T , thus T is meromorph (or has maximum analyticity). In addition T is unitary and fulfills a dispersion relation which is discussed below.

Unitarity. Starting from the optical theorem eq. 129 it follows that

$$(170) \quad \Im [T^l] = |T^l|^2$$

or for multiple channels and dropping L

$$(171) \quad \Im [T_{jj}] = \sum_{j=0}^n |T_{ij}|^2$$

$$(172) \quad \frac{i}{2}(T_{jj}^* - T_{jj}) = \sum_{j=0}^n T_{ij}^* T_{ij}.$$

Collecting terms on the left-hand side, we have

$$(173) \quad 1 - 2iT_{jj}^* + 2iT_{jj} + 4 \sum_{j=0}^n T_{ij}^* T_{ij} = 1 \sum_{j=0}^n (\delta_{ij} - 2iT_{ij}^*)(\delta_{ij} + 2iT_{ij}^*) = 1$$

This becomes equal to

$$(174) \quad \sum_{j=0}^n S_{ij}^* S_{ij} = 1$$

Since the outgoing channels are different they cannot interfere ($\langle i|j \rangle = 0$) when $i \neq j$. Therefore, we can write the unitarity condition on the S -matrix

$$(175) \quad \sum_{j=0}^n S_{kj}^* S_{ij} = \delta_{ik}$$

and obtain

$$(176) \quad \Im [T_{ij}] = \sum_n T_{nj}^* T_{ni}.$$

Dispersion Relations. The derivation of the dispersion relation requires a lot of complex variable analysis, so we present only a sketch how to obtain the relations. A detailed description can be found in [13].

From the assumption of analyticity we deduce the integral around a closed contour (C) for a point inside the contour. This is done with a Cauchy integral

$$(177) \quad T_l(s) = \frac{1}{2i\pi} \int_C \frac{T_l(s') ds'}{s' - s}$$

which can be expressed in terms of the individual parts of the contour as

$$(178) \quad T_l(s) = \frac{1}{2i\pi} \int_{-\infty}^{s_L} ds' \frac{T_l(s' + i\eta) - T_l(s' - i\eta)}{s' - s} + \frac{1}{2i\pi} \int_{(m_1+m_2)^2}^{\infty} ds' \frac{T_l(s' + i\eta) - T_l(s' - i\eta)}{s' - s} + \frac{1}{2i\pi} \left[\int_{C_0} + \int_{C_1} + \int_{C_2} \right]$$

where C_0, C_1, C_2 are the infinite circle and the small circles surrounding s_L and $(m_1 + m_2)^2$. s_L is where the left-hand cuts start and are process dependent. $(m_1 + m_2)^2$ defines the right-hand cuts (see sec. 3.5.1 for details) We have assumed η is small so that it can be neglected in the denominators. One can show that if

$$(179) \quad \begin{aligned} |T_l(s)| &\rightarrow 0 & |s| \rightarrow \infty \\ &< O((s - s_L)^{-1}) & s \rightarrow s_L \\ &< O((s - (m_1 + m_2)^2)^{-1}) & s \rightarrow (m_1 + m_2)^2 \end{aligned}$$

independently of the direction in the complex plane from which the limits are taken, then the integrals over C_0, C_1 , and C_2 make a vanishing contribution in the limit as the circles get very large or very small respectively; We shall assume this behavior to hold, as it does in analytic potential theory. Using the hermitian analyticity (e.g. $T_l(s + i\varepsilon) - T_l(s - i\varepsilon) = 2i\Im [T_l(s + i\varepsilon)]$) we have

$$(180) \quad T_l(s) = \frac{1}{\pi} \int_{-\infty}^{s_L} \frac{\Im [T_l(s')]}{s' - s} ds' + \frac{1}{\pi} \int_{(m_1 + m_2)^2}^{\infty} \frac{\Im [T_l(s')]}{s' - s} ds'$$

where the imaginary parts are evaluated at $s' + i\eta$, $\eta \rightarrow 0$ (the physical amplitude is $T_l(s + i\varepsilon)$, $\varepsilon \rightarrow 0$. s is greater than $(m_1 + m_2)^2$) which may be written

$$(181) \quad T_l(s) = \frac{1}{\pi} \int_{-\infty}^{\infty} \frac{\Im [T_l(s')]}{s' - s - i\varepsilon} ds'$$

since $\Im [T_l(s)] = 0$ between two cuts, $s_L < s < (m_1 + m_2)^2$.

3.2.5. Factorization. Eq. 142 and eq. 146 show that resonances are related to singularities of the T -matrix. The task of this section is to show that the T -matrix factorizes in the case of many open channels. From eq. 146 follows that the T -matrix has a singularity at

$$(182) \quad \cot \delta = \frac{E_R - E}{\frac{\Gamma}{2}} \Rightarrow E = E_R - i\frac{\Gamma}{2}.$$

The determinant of the inverse matrix T^{-1} has a zero at the singularity of T :

$$(183) \quad \text{Det} \left[T^{-1} \left(E = E_R - i\frac{\Gamma}{2} \right) \right] = 0$$

After diagonalization of the inverse T -matrix with a unitary matrix U we get

$$(184) \quad T_D^{-1} = \begin{pmatrix} \lambda_1 & 0 & 0 \\ 0 & \lambda_2 & 0 \\ 0 & 0 & \ddots \end{pmatrix} \Rightarrow \text{Det} [T_D^{-1}] = \lambda_1 \lambda_2 \dots$$

For a single singularity there only one Eigen-value vanishes. For a singularity of higher order several Eigen-values can be zero. For $\lambda_1 = C(E - E_R)$ we get

$$(185) \quad T_D^{-1} = \begin{pmatrix} C(E - E_R) & 0 & 0 \\ 0 & \lambda_2 & 0 \\ 0 & 0 & \ddots \end{pmatrix} \Rightarrow T_D = \begin{pmatrix} \frac{1}{C(E - E_R)} & 0 & 0 \\ 0 & \frac{1}{\lambda_2} & 0 \\ 0 & 0 & \ddots \end{pmatrix}.$$

For R_D being a matrix with

$$(186) \quad \begin{aligned} R_D &\equiv \lim_{E \rightarrow E_R} (E - E_R) T_D \\ &= \lim_{E \rightarrow E_R} \begin{pmatrix} \frac{1}{C} & 0 & 0 \\ 0 & \frac{E - E_R}{\lambda_2} & 0 \\ 0 & 0 & \ddots \end{pmatrix} = \begin{pmatrix} \frac{1}{C} & 0 & 0 \\ 0 & 0 & 0 \\ 0 & 0 & \ddots \end{pmatrix} \end{aligned}$$

the transformation

$$(187) \quad R = U^T \frac{1}{C} U \quad \text{hence} \quad R_{ij} = \sum_k U_{ik} \frac{1}{C} U_{kj}$$

proves that R can be factorized:

$$(188) \quad R_{ij} = \sum_k \frac{1}{\sqrt{C}} U_{ik} \frac{1}{\sqrt{C}} U_{kj}$$

Therefore also T can be factorized like

$$(189) \quad T_{ij} = \frac{\sqrt{\frac{\Gamma_i}{2}} \sqrt{\frac{\Gamma_j}{2}}}{E_R - E - i \sum_{r=1}^n \frac{\Gamma_R}{2}} = \frac{\sqrt{\frac{\Gamma_i \Gamma_j}{4}}}{E_R - E - i \sum_{r=1}^n \frac{\Gamma_R}{2}}.$$

3.3. *K-Matrix Formalism.* –

3.3.1. Definitions and Properties. The K -matrix formalism provides an elegant way of expressing the unitarity of the S -matrix for the processes of the type $ab \rightarrow cd$. It has been originally introduced by Wigner [14] and Wigner and Eisenbud [15] for study of resonances in nuclear reactions. The first use in particle physics goes back to an analysis of resonance production in Kp scattering by Dalitz and Tuan [16]. A comprehensive review is found in [17]. In this paper we give a concise description of the K -matrix formalism for ease of reference. Its generalizations to arbitrary production processes are covered in some detail.

The reader is referred to the text book by Martin and Spearman [12] for some of the material covered in this note. However, one must note that the definitions given in this

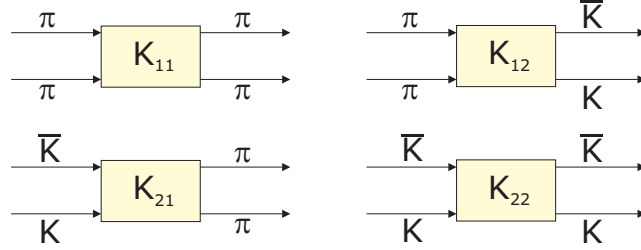


Fig. 9. – Scattering process using a K -matrix propagator. The boxes hide the actual process.

paper are different from those used by Martin and Spearman. From the unitarity of the S , one gets

$$(190) \quad T - T^\dagger = 2i T^\dagger T = 2i T T^\dagger$$

In terms of the inverse operators, eq. 190 can be rewritten

$$(191) \quad (T^\dagger)^{-1} - T^{-1} = 2iI$$

which may further be transformed into

$$(192) \quad (T^{-1} + iI)^\dagger = T^{-1} + iI.$$

One is now ready to introduce the K operator via

$$(193) \quad K^{-1} = T^{-1} + iI$$

From eq. 192 one finds that the K operator is Hermitian, i.e.

$$(194) \quad K = K^\dagger.$$

From time reversal invariance of S and T it follows, that the K operator must be symmetric, i.e. the K -matrix may be chosen to be real and symmetric. One can eliminate the inverse operators in eq. 193 by multiplying by K and T from left and right and vice versa, to obtain

$$(195) \quad T = K + iTK = K + iKT$$

which shows that K and T operators commute, i.e.

$$(196) \quad [K, T] = 0$$

and that, solving for T , one gets

$$(197) \quad T = K(I - \imath K)^{-1} = (I - \imath K)^{-1}K$$

and

$$(198) \quad S = (I + \imath K)(I - \imath K)^{-1} = (I - \imath K)^{-1}(I + \imath K).$$

Note that the T -matrix is complex only through the \imath that appears in this formula, i.e. T^{-1} has been explicitly broken up into its real and imaginary parts, see equation eq. 193.

It is also useful to split T into its real and imaginary part. From eq. 195 one finds, noting that K is a real matrix,

$$(199) \quad \Re [T] = (I + K^2)^{-1}K = K(I + K^2)^{-1}$$

$$(200) \quad \Im [T] = (I + K^2)^{-1}K^2 = K^2(I + K^2)^{-1}$$

Combining this result with eq. 190, one finds that the unitarity takes on the simple form

$$(201) \quad \Im [T] = T^*T = TT^*$$

or, from eq. 193, one gets

$$(202) \quad \Im [T^{-1}] = -I.$$

Consider now an isoscalar $\pi\pi$ scattering in S-wave below $\sqrt{s} = 1$ GeV. This is a single-channel problem and unitarity is rigorously maintained. From eq. 207, one may set

$$(203) \quad S = e^{2\imath\delta}$$

where δ is the familiar phase shift. The transition amplitude T is given, from eq. 110,

$$(204) \quad T = e^{\imath\delta} \sin \delta$$

Note that the factors 2 and \imath in eq. 110 make the T attain the simple, familiar form. This formula shows that the trajectory of T in the complex plane (Argand diagram) is a circle of a unit diameter with its center at $(0, \imath/2)$. This is the so-called unitarity circle and the physically allowed T should remain at or within this circle. The S-wave cross section is, from eq. 105,

$$(205) \quad \sigma = \left(\frac{4\pi}{q_i^2}\right) \sin^2 \delta.$$

The K -matrix for this case is simply

$$(206) \quad K = \tan \delta$$

and a pole in K is therefore associated with $\delta = \pi/2$.

Consider next a two-channel problem in which the S -matrix may be expressed as 2×2 matrices. Let S_{ij} be symmetric; then it would take six parameters to represent three complex variables: S_{11} , S_{12} , and S_{22} . The unitarity relationship

$$(207) \quad S_{ik} S_{jk}^* = \delta_{ij}$$

imposes three independent equations. This shows that the S -matrix depends on just three parameters. It can be shown readily that the matrix elements are

$$(208) \quad \begin{aligned} S_{11} &= \eta e^{2i\delta_1} \\ S_{22} &= \eta e^{2i\delta_2} \\ S_{12} &= i\sqrt{1-\eta^2} e^{i\Phi_{12}}, \quad \Phi_{12} = \delta_1 + \delta_2 \end{aligned}$$

where δ_i is the phase shift for channel i and η is the inelasticity ($\eta \leq 1$). Note that there exists only one inelasticity in the two-channel case.

Turning to the K -matrix representation of the T -matrix, let

$$(209) \quad K = \begin{pmatrix} K_{11} & K_{12} \\ K_{21} & K_{22} \end{pmatrix}$$

where $K_{12} = K_{21}$ and K_{ij} = real. Then, from eq. 193, one finds

$$(210) \quad T = \frac{1}{1 - D - i(K_{11} + K_{22})} \begin{pmatrix} K_{11} - iD & K_{12} \\ K_{21} & K_{22} - iD \end{pmatrix}$$

where

$$(211) \quad D = K_{11}K_{22} - K_{12}^2.$$

3.3.2. Lorentz-invariant Description. The transition amplitudes T as defined in eq. 110 is not Lorentz invariant. The invariant amplitude is defined through two-body wave functions for the initial and the final state, and the process of the derivation involves proper normalizations for the two-particle states (see Section 5.1, Chung [11]). The resulting invariant amplitude contains the inverse square-root of the two-body phase space elements in the initial and the final states. The Lorentz-invariant amplitude, denoted \widehat{T} , is thus given by

$$(212) \quad T_{ij} = \{\rho_i\}^{\frac{1}{2}} \widehat{T}_{ij} \{\rho_j\}^{\frac{1}{2}}.$$

In matrix notation, one may write

$$(213) \quad T = \{\rho\}^{\frac{1}{2}} \widehat{T} \{\rho\}^{\frac{1}{2}}$$

and

$$(214) \quad S = I + 2i \{\rho\}^{\frac{1}{2}} \widehat{T} \{\rho\}^{\frac{1}{2}}$$

where the phase-space ‘matrix’ is diagonal by definition, i.e.

$$(215) \quad \rho = \begin{pmatrix} \rho_1 & 0 \\ 0 & \rho_2 \end{pmatrix}$$

and

$$(216) \quad \rho_1 = \frac{2q_1}{m} \quad \text{and} \quad \rho_2 = \frac{2q_2}{m}.$$

The q_i is the breakup momentum in channel i . (Here one considers a two-channel problem for simplicity without loss of generality.) The unitarity demands that, from eq. 201 and eq. 202,

$$(217) \quad \Im [\widehat{T}] = \widehat{T}^* \rho \widehat{T} = \widehat{T} \rho \widehat{T}^*$$

and

$$(218) \quad \Im [\widehat{T}^{-1}] = -\rho$$

It is in this form one encounters most frequently the unitary conditions of the transition matrix in the literature.

The cross section in the J th partial wave is given by, from eq. 105,

$$(219) \quad \sigma_{fi}^J = \left(\frac{16\pi}{s} \right) \left(\frac{\rho_f}{\rho_i} \right) (2J+1) |\widehat{T}_{fi}^J(s)|^2$$

Note that this formula embodies the familiar presence of the flux factor of the initial system and the phase-space factor of the final system in the process $ab \rightarrow cd$. In the K -matrix formalism, one allows for ρ to become imaginary below a given threshold; however, the cross section above has no meaning below a threshold, and one could then modify the expression above by multiplying it with two step functions: $\theta(\rho_i^2)$ and $\theta(\rho_f^2)$.

One may recapitulate the expressions for the differential cross section and its partial-wave expansion in terms of the invariant amplitudes $\widehat{T}_{fi}^J(s)$. For the purpose, one defines the ‘invariant scattering amplitude’

$$(220) \quad \widehat{T}_{fi}(\Omega) = \sum_J (2J+1) \widehat{T}_{fi}^J(s) D_{\lambda\mu}^{J*}(\phi, \theta, 0)$$

and the differential cross section is given by

$$(221) \quad \frac{d\sigma_{fi}}{d\Omega} = \left(\frac{4}{s} \right) \left(\frac{\rho_f}{\rho_i} \right) |\widehat{T}_{fi}(\Omega)|^2.$$

The initial and final density of states are, with $s = m^2$,

$$(222) \quad \rho_i = \sqrt{\left[1 - \left(\frac{m_a + m_b}{m}\right)^2\right] \left[1 - \left(\frac{m_a - m_b}{m}\right)^2\right]}$$

$$(223) \quad \rho_f = \sqrt{\left[1 - \left(\frac{m_c + m_d}{m}\right)^2\right] \left[1 - \left(\frac{m_c - m_d}{m}\right)^2\right]}$$

in terms of the particle masses involved in the scattering $ab \rightarrow cd$. Note that these phase-space factors are normalized such that

$$(224) \quad \rho_i \rightarrow 1 \quad \text{as} \quad m^2 \rightarrow \infty.$$

The invariant amplitude $\widehat{T}_{fi}(\Omega)$ is dimensionless, and has a partial-wave expansion eq. 220. The partial-wave amplitude $\widehat{T}_{fi}^J(s)$ is related to the \widehat{K} -matrix via eq. 228, and unitarity is preserved if the \widehat{K} -matrix is taken to be real and symmetric. It should be noted that the formula for the differential cross section eq. 221 has no ‘arbitrary’ numerical factors. The ‘conventional’ invariant amplitude, introduced in eq. 103, is given by

$$(225) \quad \mathcal{M}_{fi} = 16\pi \widehat{T}_{fi}(\Omega)$$

One may consider again the isoscalar $\pi\pi$ scattering in S-wave below 1.0 GeV. In terms of the phase-shift δ , the invariant amplitude is given by, from eq. 204,

$$(226) \quad \widehat{T} = \frac{1}{\rho} e^{i\delta} \sin \delta$$

and when substituted into eq. 219 the cross section eq. 205 results. These expressions are very familiar, and they demonstrate clearly the interplay between the phase shifts, the invariant amplitudes and the cross sections.

One can similarly define the invariant analogue of the K -matrix through

$$(227) \quad K = \{\rho\}^{\frac{1}{2}} \widehat{K} \{\rho\}^{\frac{1}{2}}$$

translating the inverse K -matrix to (eq. 193)

$$(228) \quad \widehat{K}^{-1} = \widehat{T}^{-1} + i\rho$$

which leads to

$$(229) \quad \widehat{T} = \widehat{K} + i\widehat{K}\rho\widehat{T} = \widehat{K} + i\widehat{T}\rho\widehat{K}$$

and

$$(230) \quad \widehat{T}\rho\widehat{K} = \widehat{K}\rho\widehat{T}$$

Solving for \widehat{T} , one obtains

$$(231) \quad \widehat{T} = \widehat{K}(I - \imath\rho\widehat{K})^{-1} = (I - \imath\widehat{K}\rho)^{-1}\widehat{K}$$

and, from eq. 198,

$$(232) \quad \begin{aligned} S &= (I + \imath\{\rho\}^{\frac{1}{2}}\widehat{K}\{\rho\}^{\frac{1}{2}})(I - \imath\{\rho\}^{\frac{1}{2}}\widehat{K}\{\rho\}^{\frac{1}{2}})^{-1} \\ &= (I - \imath\{\rho\}^{\frac{1}{2}}\widehat{K}\{\rho\}^{\frac{1}{2}})^{-1}(I + \imath\{\rho\}^{\frac{1}{2}}\widehat{K}\{\rho\}^{\frac{1}{2}}). \end{aligned}$$

Note that \widehat{K} and ρ do not commute. The Lorentz-invariant T -matrix is then given by

$$(233) \quad \widehat{T} = \frac{1}{1 - \rho_1\rho_2\widehat{D} - \imath(\rho_1\widehat{K}_{11} + \rho_2\widehat{K}_{22})} \begin{pmatrix} \widehat{K}_{11} - \imath\rho_2\widehat{D} & \widehat{K}_{12} \\ \widehat{K}_{21} & \widehat{K}_{22} - \imath\rho_1\widehat{D} \end{pmatrix}$$

where

$$(234) \quad \widehat{D} = \widehat{K}_{11}\widehat{K}_{22} - \widehat{K}_{12}^2.$$

3.3.3. Implementation of Dynamics (and/or Resonances). There are two possibilities for parameterizing resonances in K -matrix formalism: Resonances can arise from constant K -matrix elements with the energy variation supplied by phase space or from strongly varying K -matrix elements (pole terms) supplying a phase motion [24]. They differ in their dynamical character. The former are assumed to arise from exchange forces in the corresponding hadronic channels (molecular resonances), so that great effects are expected near corresponding thresholds, whereas the latter (normal resonances) correspond to dynamical sources at the constituent level, coupling to the observed hadrons through decay [24]. The dynamical origin of resonances has to be determined by experiment. In the approximation of resonance domination for the amplitudes, one has therefore

$$(235) \quad K_{ij} = \sum_R \frac{g_{Ri}(m)g_{Rj}(m)}{m_R^2 - m^2} + c_{ij}$$

and

$$(236) \quad \widehat{K}_{ij} = \sum_R \frac{g_{Ri}(m)g_{Rj}(m)}{(m_R^2 - m^2)\sqrt{\rho_i\rho_j}} + \hat{c}_{ij}$$

where the sum on R goes over the number of poles with masses m_R , and the residue functions (expressed in units of energy) are given by

$$(237) \quad g_{Ri}^2(m) = m_R\Gamma_{Ri}(m)$$

where $g_{Ri}(m)$ is real (but it could be negative) above the threshold for channel i . The constant K -matrix elements have to be dimensionless and real to preserve unitarity. The corresponding width $\Gamma_R(m)$ is

$$(238) \quad \Gamma_R(m) = \sum_i \Gamma_{Ri}(m)$$

for each pole R .

Consider now a normal resonance R coupling to n open two-body channels, i.e. the mass m_R is above the threshold of all the two-body channels. The partial widths may be given an expression

$$(239) \quad \Gamma_{Ri}(m) = \frac{g_{Ri}^2(m)}{m_R} = \gamma_{Ri}^2 \Gamma_R^0 [B_{Ri}^l(q, q_R)]^2 \rho_i$$

and the residue function by

$$(240) \quad g_{Ri}(m) = \gamma_{Ri} \sqrt{m_R \Gamma_R^0} B_{Ri}^l(q, q_R) \sqrt{\rho_i}.$$

The $B(m)$'s are ratios of usual centrifugal barrier factors in terms of the breakup momentum in channel i and the resonance breakup momentum q_R for the orbital angular momentum l :

$$(241) \quad B_{Ri}^l(q, q_R) = \frac{F_l(q)}{F_l(q_R)}$$

Widely used are Blatt-Weisskopf barrier factors [22] (see 3.2.3) for more details. The γ 's are real constants (but they can be negative) and may be given the normalization

$$(242) \quad \sum_i \gamma_{Ri}^2 = 1.$$

In practice, it is probably better to avoid this normalization condition by using the parameters

$$(243) \quad g_{Ri}^0 = \gamma_{Ri} \sqrt{m_R \Gamma_R^0}$$

as variables in the fit. The residue function is then given by

$$(244) \quad g_{Ri}(m) = g_{Ri}^0 B_{Ri}^l(q, q_R) \sqrt{\rho_i}.$$

We define a K -matrix total width $\tilde{\Gamma}_R$ and the K -matrix partial widths $\tilde{\Gamma}_{Ri}$ by

$$(245) \quad \tilde{\Gamma}_R = \sum_i \tilde{\Gamma}_{Ri} = \Gamma_R(m_R) = \Gamma_R^0 \sum_i \gamma_{Ri}^2 \rho_i(m_R)$$

From these one finds

$$(246) \quad \Gamma_R^0 = \sum_i \frac{\tilde{\Gamma}_{Ri}}{\rho_i(m_R)},$$

$$(247) \quad \gamma_{Ri}^2 = \frac{\tilde{\Gamma}_{Ri}}{\Gamma_R^0 \rho_i(m_R)},$$

$$(248) \quad g_{Ri}^0 = \sqrt{\frac{m_R \tilde{\Gamma}_{Ri}}{\rho_i(m_R)}}.$$

Note that the K -matrix width do not need to be identical with the width which is observed in an experimental mass distribution nor with the width of the \hat{T} -matrix pole in the complex energy plane. We will refer the former as Γ_{obs} , the latter as Γ_{pole} . In the limit in which the masses of the decay particles can be neglected compared to m_R , one has $\Gamma_R(m_R) \simeq \Gamma_R^0$.

In terms of the γ 's and g^0 's, the invariant K -matrix now has a simpler form

$$(249) \quad \begin{aligned} \hat{K}_{ij} &= \sum_R \frac{\gamma_{Ri} \gamma_{Rj} m_R \Gamma_R^0 B_{Ri}^l(q, q_R) B_{Rj}^l(q, q_R)}{m_R^2 - m^2} \\ &= \sum_R \frac{g_{Ri}^0 g_{Rj}^0 B_{Ri}^l(q, q_R) B_{Rj}^l(q, q_R)}{m_R^2 - m^2} \end{aligned}$$

allowing for the possibility that γ 's and g^0 's can be negative.

Consider now an isovector P -wave $\pi\pi$ scattering at or near the ρ mass. Then the $\pi\pi$ elastic scattering amplitude is given by

$$(250) \quad K = \frac{m_0 \Gamma(m)}{m_0^2 - m^2} = \tan \delta$$

where m_0 is the mass of the ρ and δ is the usual phase shift. The mass-dependent width is given by

$$(251) \quad \Gamma(m) = \tilde{\Gamma}_0 \left(\frac{\rho}{\rho_0} \right) [B^1(q, q_0)]^2$$

where $\tilde{\Gamma}_0$ is the K -matrix width and q (q_0) is the $\pi\pi$ break-up momentum for the $\pi\pi$ mass m (m_0). Neglecting the angular dependence of the amplitude, one obtains

$$(252) \quad T = e^{i\delta} \sin \delta = \left[\frac{m_0 \tilde{\Gamma}_0}{m_0^2 - m^2 - im_0 \Gamma(m)} \right] [B^1(q, q_0)]^2 \left(\frac{\rho}{\rho_0} \right)$$

The first bracket in eq. 252 contains the usual Breit-Wigner form and the last bracket expresses the two-body phase-space factor. In this simple case, the K -matrix width

and the observed width are identical. Note that the phase-space factor is absent in the Lorentz-invariant amplitude \widehat{T} given by eq. 212. The q^2 dependence of the amplitude (in $[B^1(q, q_0)]^2$) reflects the fact that both the initial and the final $\pi\pi$ systems are in P -wave. The normalization for the transition amplitude has been chosen such that

$$(253) \quad T = +i \quad \text{and} \quad \widehat{T} = \frac{+i}{\rho} \quad \text{at} \quad m = m_0.$$

It is seen that the invariant amplitude \widehat{T} is not normalized to 1 but to ρ^{-1} . It is for this reason that the Argand diagram is usually plotted with T and not \widehat{T} .

3.3.4. Some Examples.

Coupled Channel Case. In this example we investigate the influence of coupling of a resonance to a second open channel at the T -matrix parameters (phase-shift δ and inelasticity η). Consider an S -wave resonance at $1500 \text{ MeV}/c^2$ decaying into $\pi\pi$ and $K\bar{K}$ with a total width of $100 \text{ MeV}/c^2$. In the first example we have chosen the K -matrix widths to be $\tilde{\Gamma}_{\pi\pi} = 20 \text{ MeV}/c^2$ and $\tilde{\Gamma}_{K\bar{K}} = 80 \text{ MeV}/c^2$; in the second one we choose $\tilde{\Gamma}_{\pi\pi} = 80 \text{ MeV}/c^2$ and $\tilde{\Gamma}_{K\bar{K}} = 20 \text{ MeV}/c^2$. The change of the coupling to the channel $K\bar{K}$ has no influence on the inelasticity η and on the line shape of $|T|^2$. The only visible difference is the behavior of the phase motion δ (see fig. 10(b)). In the case of a strong coupling to the $K\bar{K}$ channel ($\tilde{\Gamma}_{K\bar{K}} = 80 \text{ MeV}/c^2$) one cannot decide whether there is a resonance or not by measuring the first channel only (here $\pi\pi$), if the errors of the phase-shift are large. Note the different scales for the phase-shift δ for the two examples.

Nearby Resonances. Consider again a $\pi\pi$ scattering at mass m . But suppose there exist two resonances with masses m_a and m_b coupling to the isoscalar D -wave channel. The prescription for the K -matrix in this case is that

$$(254) \quad K = \frac{m_a \Gamma_a(m)}{m_a^2 - m^2} + \frac{m_b \Gamma_b(m)}{m_b^2 - m^2}$$

i.e. the poles are summed in the K -matrix. The mass-dependent widths are given by

$$(255) \quad \Gamma_R(m) = \tilde{\Gamma}_R^0 \left(\frac{m_a}{m} \right) \left(\frac{q}{q_R} \right) [B^2(q, q_R)]^2$$

where $r = a$ or $r = b$ and $\tilde{\Gamma}_a^0$ and $\tilde{\Gamma}_b^0$ are the two observed widths in the problem. q_r is the $\pi\pi$ breakup momentum at $m = m_r$. If m_a and m_b are far apart relative to the widths, then K is dominated either by the first or the second resonance depending on whether m is near m_a or m_b . The transition amplitude is then given merely by the sum

$$(256) \quad T \simeq \left[\frac{m_a \tilde{\Gamma}_a^0}{m_a^2 - m^2 - i m_a \Gamma_a(m)} \right] \left[\left(\frac{m_a}{m} \right) \left(\frac{q}{q_a} \right) \right] [B^2(q, q_a)]^2$$

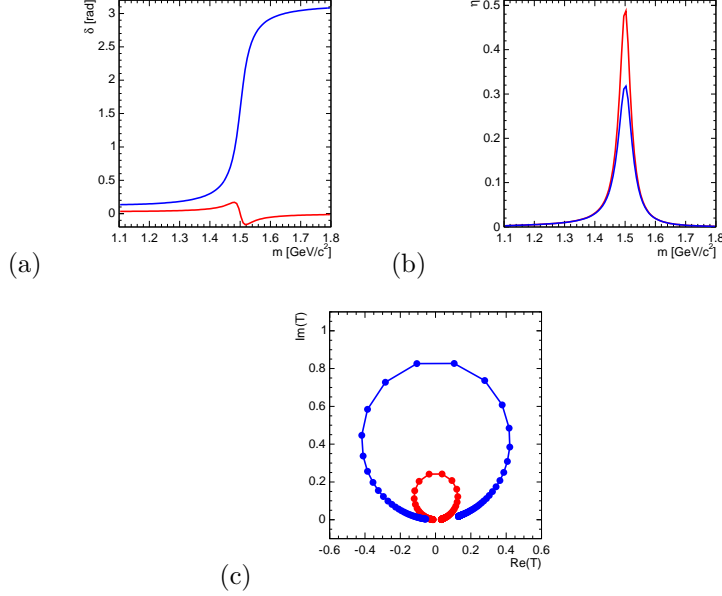


Fig. 10. $-\pi\pi$ dominated decays of a resonance at $1500 \text{ MeV}/c^2$ with a total width of $100 \text{ MeV}/c^2$. (light curve $K\bar{K}$ dominates, black curve $\pi\pi$ dominates). In the case of a dominant $\pi\pi$ width, the phase (a) looks normal in $\pi\pi$, while it changes dramatically and gets tiny if the $K\bar{K}$ channel dominates. (b) shows the line shape and (c) the Argand plot for both channels

$$(257) \quad + \left[\frac{m_b \tilde{\Gamma}_b^0}{m_b^2 - m^2 - im_b \Gamma_b(m)} \right] \left[\left(\frac{m_b}{m} \right) \left(\frac{q}{q_b} \right) \right] [B^2(q, q_b)]^2.$$

In the limit in which the two states have the same mass, i.e. $m_0 \equiv m_a = m_b$, then the transition amplitude becomes

$$(258) \quad T = \frac{m_0 [\Gamma_a(m) + \Gamma_b(m)]}{m_0^2 - m^2 - im_0 [\Gamma_a(m) + \Gamma_b(m)]}.$$

This shows that the result is a single Breit-Wigner form but its total width is now the sum of the two individual widths. In case of two nearby resonances eq. 257 is not strictly valid. For a specific example fig. 11 shows the transition amplitude T from the correct equation eq. 254 and from the approximate eq. 257. Note that eq. 257 exceeds the unitary circle.

Flatté Formula. As a next example we take the isovector S -wave scattering with the $a_0(980)$ coupling to the $\pi\eta$ (channel 1) and $K\bar{K}$ (channel 2) final states. Then the

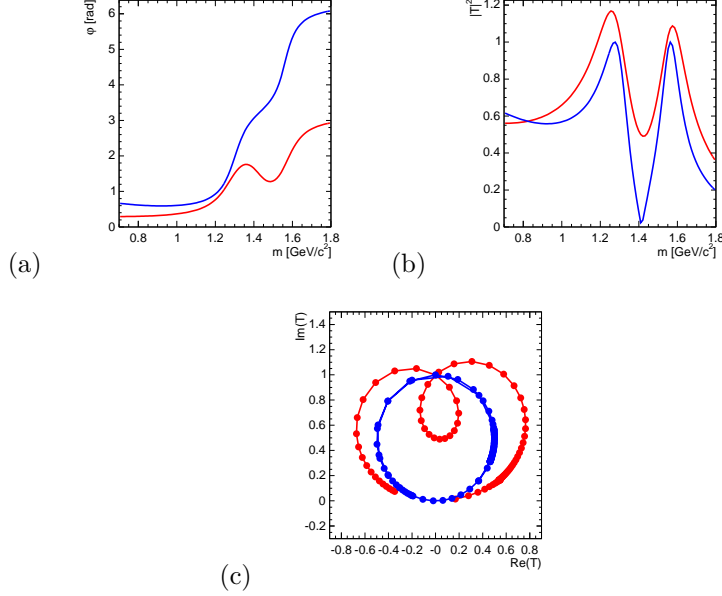


Fig. 11. – Nearby resonances in K -matrix formalism compared to sum of Breit-Wigner. The light curves show the sum of Breit-Wigner functions and the black curves demonstrate the effect of a unitarized K -matrix approach. The masses are $m_a=1.275 \text{ MeV}/c^2$, $\Gamma_a^0=185 \text{ MeV}/c^2$ and $m_a=1.565 \text{ MeV}/c^2$, $\Gamma_a^0=150 \text{ MeV}/c^2$. Both resonances decay only to $\pi\pi$. It is clearly visible how the sum of Breit-Wigner functions violate unitarity (c), while the K -matrix formalism leads to a nice circle. The effect is also visible in the phases (a) which moves backward for while and in the intensity (b) where it exceeds unity.

elements of the invariant K -matrix eq. 249 are

$$(259) \quad \hat{K}_{11} = \frac{\gamma_1^2 m_0 \Gamma_0}{m_0^2 - m^2}$$

$$(260) \quad \hat{K}_{22} = \frac{\gamma_2^2 m_0 \Gamma_0}{m_0^2 - m^2}$$

$$(261) \quad \hat{K}_{12} = \hat{K}_{21} = \frac{\gamma_1 \gamma_2 m_0 \Gamma_0}{m_0^2 - m^2}.$$

The normalized couplings are denoted by γ_1^2 and γ_2^2 , which are both dimensionless and satisfy

$$(262) \quad \gamma_1^2 + \gamma_2^2 = 1.$$

Then the \widehat{T} -matrix eq. 233 is given as

$$(263) \quad \widehat{T} = \frac{m_0 \Gamma_0}{m_0^2 - m^2 - i m_0 \Gamma_0 (\rho_1 \gamma_1^2 + \rho_2 \gamma_2^2)} \begin{pmatrix} \gamma_1^2 & \gamma_1 \gamma_2 \\ \gamma_1 \gamma_2 & \gamma_2^2 \end{pmatrix}$$

If one sets eq. 243

$$(264) \quad g_i = \gamma_i \sqrt{m_0 \Gamma_0}$$

so that

$$(265) \quad g_1^2 + g_2^2 = m_0 \Gamma_0$$

then

$$(266) \quad \widehat{T} = \frac{\begin{pmatrix} g_1^2 & g_1 g_2 \\ g_1 g_2 & g_2^2 \end{pmatrix}}{m_0^2 - m^2 - i (\rho_1 g_1^2 + \rho_2 g_2^2)}.$$

This is the Flatté formula [23].

The $a_0(980)$ appears as a ‘regular’ resonance in the $\pi\eta$ system (channel 1). The comparable Breit-Wigner denominator, for m near m_r , is $m_r^2 - m^2 - i m_r \Gamma_r$ in the resonance approximation. One finds, therefore,

$$(267) \quad m_0^2 = m_r^2 + \left(\frac{\gamma_2}{\gamma_1}\right)^2 \left[\frac{|\rho_2(m_r)|}{\rho_1(m_r)} \right] m_r \Gamma_r$$

$$(268) \quad \Gamma_0 = \frac{m_r \Gamma_r}{m_0 \rho_1(m_r) \gamma_1^2}$$

in terms of the mass m_r and width Γ_r . Note that ρ_i ’s have been evaluated at $m = m_r$ where \widehat{T} is expected to attain its maximum value. The above formulas give merely a good starting point; in practice one must vary m_0 and Γ_0 to fit the $\pi\eta$ spectrum. The ratio $(\gamma_2/\gamma_1)^2$ is an unknown (commonly fixed at the $SU(3)$ value of 1.5), but the shape of the square of the amplitudes depends only weakly on this value. Once the ratio is fixed, then γ_1^2 and γ_2^2 are fixed through the normalization condition eq. 262. Now we turn to few examples how K -matrices have actually been used in various analysis.

Example: $\pi\pi$ S-Wave á la Au, Morgan and Pennington. [24] The work from Au, Morgan and Pennington combines most of the data on $\pi\pi$ and $K\bar{K}$ scattering at that time. For the $I = \pi\pi$ S-wave the following parametrization was chosen

$$(269) \quad K_{ij} = \frac{s - s_0}{4m_K^2} \sum_r \frac{g_{r,i} g_{r,j}}{(s_r - s)(s_r - s_0)} + \sum_n c_{ij}^n \left[\frac{s}{4m_K^2} - 1 \right]$$

$$(270) \quad \equiv (s - s_0) \widehat{K}_{ij}$$

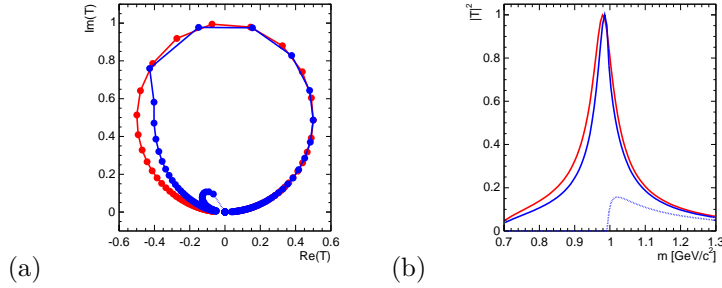


Fig. 12. – Difference between Flatté and Breit-Wigner. (a) The Breit-Wigner function (grey curve) shows a unit circle, while in the Flatté function (black curves) one sees in channel 1 a drop in elasticity at threshold of channel 2 and a small circle for channel 2 starting at the respective threshold. (b) Interestingly the line shape for channel 1 does not change very much, while for channel 2 there is a dramatic effect at threshold.

Alternatively they parametrize also an M -matrix. The M -matrix approach is defined by $T = (M - i\rho)^{-1}$. They use

$$(271) \quad M_{ij} = \frac{a_{ij}}{s - s_0} + \sum_r \frac{g'_{r,i} g'_{r,j}}{s'_r} + \sum_n c'_{ij} \left[\frac{s}{4m_K^2} - 1 \right]$$

As we will see in most parameterizations of the $\pi\pi$ S -wave a parameter like s_0 appears to satisfy the condition of the Adler zero.

Example: $\pi\pi$ S -Wave á la Crystal Barrel. This parametrization was used to analyze the Crystal Barrel data of the channels $\bar{p}p \rightarrow 3\pi^0$, $2\pi^0\eta$ and $2\eta\pi^0$ with an open $K\bar{K}$

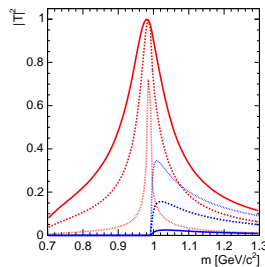


Fig. 13. – Effect of coupling variations in the Flatté formula. The stronger the coupling the more dramatic are the effects on the line shape. The solid, dashed and dotted curves represent coupling ratios from $\gamma_1^2/\gamma_2^2=10$ to 1 and 0.1. respectively for the two channels.

channel [25] being constrained by scattering data [26, 27]. A K -Matrix formalism was applied using

$$(272) \quad K_{ij} = \sum_r \frac{g_{r,i} g_{r,j} B_i^l(q_i) B_j^l(q_j)}{m_r^2 - m^2} + c_{ij}$$

with K being a 3×3 matrix with the channels $1 = \pi\pi$, $2 = K\bar{K}$ and $3 = \eta\eta$. The centrifugal barrier was chosen according to the work of Hippel and Quigg [22]. For scalars this factor is equal to one.

Example: $\pi\pi$ S-Wave á la Anisovich and Sarantsev. The work of Anisovich and Sarantsev is the most sophisticated so far and combines all Crystal Barrel data as well as scattering data and other information. The parametrization is very complex and involves a lot of parameters to accommodate the different reactions [28].

$$(273) \quad K_{ij}(s) = \left(\sum_r \frac{g_{r,i} g_{r,j}}{m_r^2 - s} + f_{ij} \frac{s_1 + s_0}{s + s_0} \right) \frac{s - s_A}{s + s_{A0}}$$

where K_{ij} is a 5×5 matrix ($i, j = 1, 2, 3, 4, 5$), with the following notations for meson states: $1 = \pi\pi$, $2 = K\bar{K}$, $3 = \eta\eta$, $4 = \eta\eta'$ and $5 =$ multi-meson states (like dominant four-pion state for $s < 1.6 \text{ GeV}/c^2$). The $g_{r,i}$ is the coupling constant of the bare state r to a particular channel i . The parameters f_{ij} and s_0 describe a smooth part of the K -matrix elements. The factor $(s - s_A)/(s - s_{A0})$ is used to suppress the false kinematic singularity at $s = 0$ in the physical region near the $\pi\pi$ threshold. The parameters s_A and s_{A0} are kept to be small.

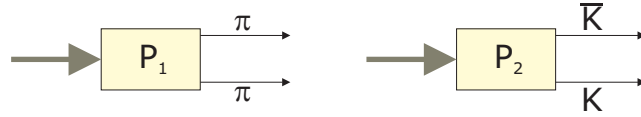


Fig. 14. – Production process. The boxes hide the actual process. The source of production is unknown and therefore replaced by a strength parameter.

3.4. P -Vector Approach. – So far one has considered s -channel resonances, or ‘formation’ of resonances, observed in the two-body scattering of the type $ab \rightarrow cd$. The K -matrix formalism can be generalized to cover the case of ‘production’ of resonances in more complex reactions. The key assumption is that the two-body system in the final state is an isolated one and that the two particles do not simultaneously interact with the rest of the final state in the production process.

According to Aitchison [29], the production amplitude P should be transformed into F in the presence of two-body final state interactions, as follows:

$$(274) \quad F = (I - iK)^{-1} P = TK^{-1} P$$

Or, taking the invariant form, it may be written

$$(275) \quad \widehat{F} = (I - i\widehat{K}\rho)^{-1}\widehat{P} = \widehat{T}\widehat{K}^{-1}\widehat{P}$$

where \widehat{P} characterizes production of a resonance and \widehat{F} is the resulting invariant amplitude. Note the following relationships:

$$(276) \quad F = \{\rho\}^{\frac{1}{2}}\widehat{F} \quad \text{and} \quad P = \{\rho\}^{\frac{1}{2}}\widehat{P}$$

Consider first a single-channel problem, e.g. the isoscalar $\pi\pi$ system in S -wave below $K\bar{K}$ threshold. Then, the K is simply given by eq. 206 and one finds

$$(277) \quad \widehat{F} = e^{i\delta} \cos \delta \widehat{P}.$$

Unitarity demands that in this case the phase of the total amplitude \widehat{F} and the $\pi\pi$ scattering phase δ should be identical. Thus the final-state interaction brings in a factor $e^{i\delta}$ —this is the familiar Watson's theorem [30] and the production amplitude \widehat{P} has to be a real function. It is emphasized that \widehat{P} must have the same poles as those of the K -matrix; otherwise \widehat{F} would vanish at the pole position ($\delta = \pi/2$).

In general, \widehat{P} and \widehat{F} are both column vectors, n -dimensional for an n -channel problem. If the K -matrix is given as a sum of the poles as in eq. 235, then the corresponding P -vector is

$$(278) \quad P_i = \sum_R \frac{\beta_R^0 g_{Ri}(m)}{m_R^2 - m^2}$$

and

$$(279) \quad \widehat{P}_i = \sum_R \frac{\beta_R^0 g_{Ri}(m)}{(m_R^2 - m^2)\sqrt{\rho_i}}$$

where β_R^0 (expressed in units of energy), carries the production information of the resonance R . The constant β_R^0 is in general complex, but it can be set to be real under certain assumptions. One should note, that Longacre [31, 32, 33] used complex β throughout his analysis. This ansatz was heavily criticized by Morgan and Pennington [20]

The P -vector should contain the same set of poles as those found in the K -matrix. However, according to Aitchison, constant terms (or a polynomial in energy) can always be added to the poles in the P -vector (as in the K -matrix) elements, without destroying the unitarity of the F -vector (or T -matrix),

$$(280) \quad P_i \rightarrow P_i + d_i$$

where the constant d_i is in general complex.

In [34] the production process $p\bar{p} \rightarrow \pi^+\pi^-\pi^0$ was described by a production amplitude for the ρ $\pi\pi$ and $f_2(1270)$ $\pi\pi$ intermediate states. The data required introduction of

an additional constant amplitude which was interpreted as that for direct three-pion production. This direct production amplitude can be described in our formalism with an additional constant in the F -vector.

It is often more convenient to rescale β^0 's

$$(281) \quad \beta_R^0 = \beta_R \sqrt{m_R \Gamma_R^0}$$

so that β 's are dimensionless. Then the \widehat{P} -vector reads, from eq. 243, eq. 244,

$$(282) \quad \widehat{P}_i = \sum_R \frac{\beta_R \gamma_{Ri} m_R \Gamma_R^0 B_{Ri}^l(q, q_R)}{m_R^2 - m^2}$$

where, once again, γ 's are real but β 's could be complex. If the production process has some known dependence on momentum or angular momentum, the production strength β should be modified accordingly.

It is instructive to work out the above formula in the case of a single resonance in a single channel. Then one has $\widehat{P} = \frac{\beta m_0 \Gamma_0}{m_0^2 - m^2} B^l(q, q_0)$ so that, with $\widehat{K} \rho$ given by eq. 250,

$$(283) \quad \widehat{F}(m) = \beta \frac{m_0 \Gamma_0}{m_0^2 - m^2 - i m_0 \Gamma(m)} B^l(q, q_0).$$

This is exactly what one writes down for a Breit-Wigner form, except that one has multiplied by an arbitrary constant β and the centrifugal damping factor $B^l(q, q_0)$. This provides a K -matrix justification of the traditional 'isobar' model. Note that the numerator is a constant (independent of m).

The scattering process may involve particle exchange in the t -channel (see fig. 15) and the left-hand singularities reach into the physical region. Since the formalism does not have any left-hand-cuts, they lead to artificial poles in a P -vector approach. Since these artificial poles depend on the physical processes involved and differ from reaction to reaction. If such poles exist, they can be different in the definition of the K -matrix and the P -vector.

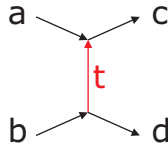


Fig. 15. – t -Channel scattering.

Cahn and Landshoff [18] state that in some approximations the column vector

$$(284) \quad Q = K^{-1}P \quad \text{and} \quad \{\rho\}^{\frac{1}{2}}Q = \widehat{Q} \quad \text{and} \quad \widehat{Q} = \widehat{K}^{-1}\widehat{P}$$

may be considered a constant in a given limited energy range. Then, one has

$$(285) \quad F = TQ \quad \text{and} \quad \widehat{F} = \widehat{T}\widehat{Q}$$

i.e. the two-body final-state interaction may be expressed as a product of the \widehat{T} -matrix and a constant column vector. The \widehat{Q} -vector is devoid of the threshold singularities (i.e., no dependence on ρ) and does not contain pole terms. It therefore depends in general on $s = m^2$ only. In a single-channel problem, e.g. the isoscalar $\pi\pi$ system in S -wave below 1 GeV, we now obtain, instead of eq. 277 derived for the P vector approach:

$$(286) \quad \widehat{F} = \frac{1}{\rho} e^{i\delta} \sin \delta \widehat{Q}$$

This amplitude contains the familiar scattering amplitude $e^{i\delta} \sin \delta$.

The P - and Q -vector approaches, even though both being approximations for production of multi particle final states, correspond to different interpretations of the physical processes. For clarity we consider a specific reaction, e.g. channel 1: $\bar{p}p \rightarrow \pi\pi\eta$ and channel 2: $\bar{p}p \rightarrow K\bar{K}\eta$ from which we want to extract information on $(\pi\pi)$ interactions. In the Q -vector approach, the amplitude is given by $F_1 = T_{11}Q_1 + T_{12}Q_2$: the $\pi\pi$ system is produced with an amplitude $Q_1(s)$. The two-pion interactions are then taken into account by the scattering amplitude T_{11} . Alternatively, a K and a \bar{K} are produced with amplitudes Q_2 which scatter via T_{12} into the outgoing pions. This picture has to be contrasted to that which one may have in mind in applying the P -vector approach, $F = (I - iK)^{-1}P$. A resonance is produced with an amplitude P , the term $(I - iK)^{-1}$ may be considered as propagator for this particle which then decays.

3.5. N/D -Method by Example. – The parametrization in terms of K -matrices with or without production vectors is only one approach to describe two-body scattering. Under the assumption of unitarity and maximum analyticity it is possible to derive the N/D method from the dispersion relations. The amplitude T_l for a given angular momentum fulfills a dispersion relation derived from the optical theorem. This is an integral equation for which has no explicit solution. But T_l can be expressed in terms of a nominator N_l and a denominator D_l

$$(287) \quad T_l(s) = \frac{N_l(s)}{D_l(s)}$$

where N_l contains only left-side singularities and D_l only right-side singularities. The functions N_l and D_l are correlated by a system of integral equations. The advantage is, that this system can be reduced to a differential equation of the the Fredholm type, which is known to be solvable. The solution is a infinite series, where the actual form depend on the integration kernel. In practice this method is realized by a finite sum, with parameters being tuned to fit the experimental data.

The work by Anisovich, Bugg, Sarantsev and Zou [35] may serve as an example for such an analysis. In order to fit the Crystal barrel data on $\bar{p}p \rightarrow 3\pi^0$, and $2\eta\pi^0$ they

used the following Ansatz below $1.1 \text{ GeV}/c^2$

$$\begin{aligned}
 K_{ij} &= \left(\frac{s - 2m_\pi^2}{s} \right) \left(\frac{\alpha_i \alpha_j}{s_A - s} \frac{\beta_i \beta_j}{s_B - s} \frac{\gamma_i \gamma_j}{s_C - s} + a_{ij} + b_{ij} s \right) \\
 (288) \quad N_{\pi\pi}(s) &= N_{11}(s) = (c_1 + c_2 s) K_{11} + i\rho_2 (c_3 + c_4 s) (K_{11} K_{22} - K_{12} K_{21}) \\
 N_{\eta\eta}(s) &= N_{22}(s) = c_1 K_{22} + i\rho_2 c_3 (K_{11} K_{22} - K_{12} K_{21})
 \end{aligned}$$

where ρ_i are the usual phase space factors and a_{ij} , b_{ij} and c_i are arbitrary complex parameters and s_i are pole positions. $\alpha_i, \dots, \gamma_i$ are coupling constants.

3.5.1. What is a Resonance. So far we collected several approaches to obtain a dynamical function. But all formalisms are only parameterizations which are more or less motivated by models. The main physical content is hidden in the T -matrix, however it was obtained.

The instructive Breit-Wigner function is well suited for low statistics, where complicated methods fail because of the many unconstrained parameters, or in the case of very well separated resonances. In this case the fitted mass and width are easily mapped to the physical properties of the state. In general this is more complicated and lead s to the investigation of the singularities of the meromorph T -matrix.

The K -matrix poles as well as other parameterization deliver only in rare cases singularities which are near to them of the T -matrix. This is for example the case for

- resonances which are very far apart,
- minimal coupling to sub-dominant channels and
- far away from thresholds.

If at least one of those is violated interference terms appear which move the unphysical poles.

	Sheet	$\Im [q_1]$	$\Im [q_2]$
I		+	+
II		-	+
III		-	-
IV		+	-

TABLE II. – *Definition of Riemann sheets (2 channels).*

The energy of a particle is function of p^2 . The inverse function, the root, has no unique solution. The sign can be positive or negative. If the momentum is a complex number, the two roots lie π apart on the same circle. This is easily illustrated for $w = z^2$. If $z = e^{i\varphi}$ then $w = e^{2i\varphi}$. If φ moves only from 0 to π then w moves around the whole

circle. If φ moves on w starts a second turn. The difference between the lower and upper function value is

$$(289) \quad \sqrt{w} - \sqrt{w^*} = \pm \sqrt{|w|} \left(e^{i\frac{\varphi}{2}} + e^{-i\frac{\varphi}{2}} \right) = \cosh \frac{\varphi}{2} \Big|_{\varphi=0} \neq 0.$$

To resolve this ambiguity one introduces for each threshold involved in the process a new pair of Riemann sheets, which represent each one possible root of the breakup momentum. The convention is (1) that every crossing of the real energy axis involves a sign change for the open channel and (2) that for every passed threshold the sign of the threshold channel changes. Please see tbl. II and fig. 16 for illustration. This means for a two channel problem

$$(290) \quad (\hat{T}^{III})^{-1} = (\hat{T}^{II})^{-1} + i\rho_2$$

where (III) and (II) denote Riemann sheets according to the definitions in tbl. II. The

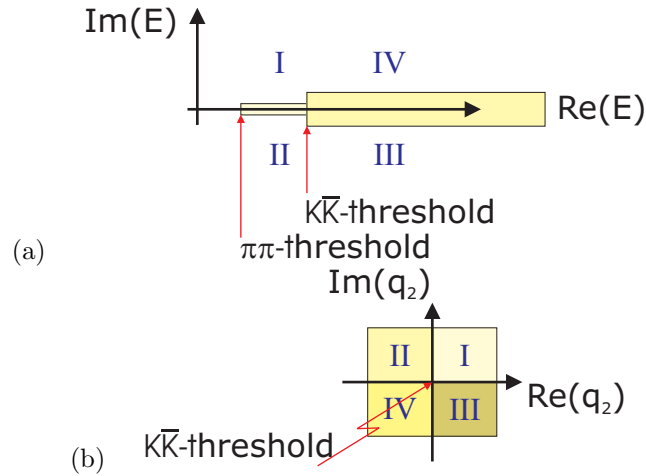


Fig. 16. – Numbering of Riemann-sheets (2 channels).

different sheets in the complex energy and momentum plane are shown in fig. 16. The different sheets are separated by cuts. The convention is that the cuts lie on the real axis and start at the threshold. In s -channel it is common to define the real axis above the threshold to be the right-hand cut (RHC). It contains all singularities of the s -channel scattering processes. The t - and u -channel can have resonances and bound-states too, which depend upon the reaction under investigation and are defined as left-hand cuts (LHC), since they appear usually below threshold (see fig. 17 for illustration). One should note, that these singularities are not taken into account in K -matrix formalisms. Furthermore, the LHC may reach far out into the physical region, where they might

imitate resonances. This has dramatic effects for the interpretation of poles in a transition

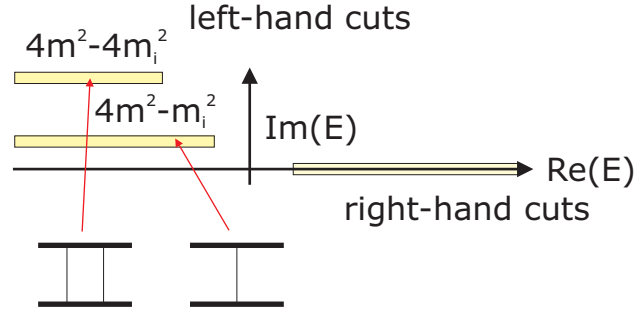


Fig. 17. – Illustration of left-hand and right-hand cuts.

amplitude. To clearly identify resonances it is mandatory to investigate the convergence radius of the pole. The convergence radius has to reach out to the real axis. Unfortunately the amplitude on the real axis is dominated by the nearest singularity and effects from the LHC if they influence the physical region. In summary this means, that the question of resonances is translated into the question of how many poles does the T -matrix have in the complex energy plane and what are their properties.

The basic idea is simple. The T -matrix contains a complex denominator D . A singularity appears if D vanishes. The mass of a resonance is then the real part of this point and the width is twice the imaginary part

$$(291) \quad T\left(E + i\frac{\Gamma}{2}\right) = 0$$

which has a similar singularity as a non-relativistic Breit-Wigner. The fundamental statement is fact that the relation between the position of the pole and the according Riemann sheet characterize the resonance [20]. The cross section (real axis) is mainly influenced by the nearest pole (see fig. 18). In principle all poles influence the real axis, which is easily seen if they are close together. In general the following approximation holds near the threshold (at the boundary between sheets II and III)

$$(292) \quad \Gamma_r^{\text{BW}} \approx \frac{1}{2} (\Gamma_r^{\text{II}} + \Gamma_r^{\text{III}})$$

where Γ_r^{III} is usually larger than Γ_r^{II} . The empirical principle of meromorph functions for T (maximum analyticity or analytic with a finite number of poles) requires that only physical singularities are allowed in the analytic continuation into the complex energy and momentum plane like

- kinematic singularities which are defined via unitarity relations. They appear at every threshold, where the two-body breakup gets real,

- dynamic singularities due to the interaction, like in exchange processes, and
- poles which correspond to resonances or bound states.

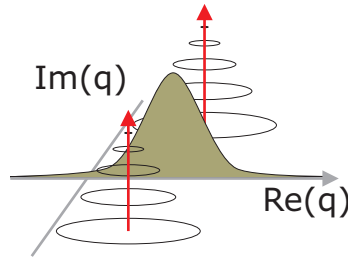


Fig. 18. – From a pole to a real Breit-Wigner. The nearest pole dominates the properties of a point on the real axis.

The time dependence of a decay amplitude is the Fourier transform of an exponential decay ($\propto e^{iq_r t}$). Thus, the imaginary part of q_r is negative, which means, that the pole lies in the unphysical half of the momentum plane ($\Im [q] < 0$, see fig. 19a). In contrast to that, a bound state lies on the positive imaginary axis. Due to unitarity and hermitian analyticity the analytic continuation leads to

$$(293) \quad \hat{T}_l(q) = \hat{T}_l^*(-q^*) \quad \text{and} \quad \hat{T}_l(s) = \hat{T}_l^*(s^*).$$

Therefore we have two poles for a resonance symmetric around the imaginary axis. In the energy plane they lie symmetric around the real axis.

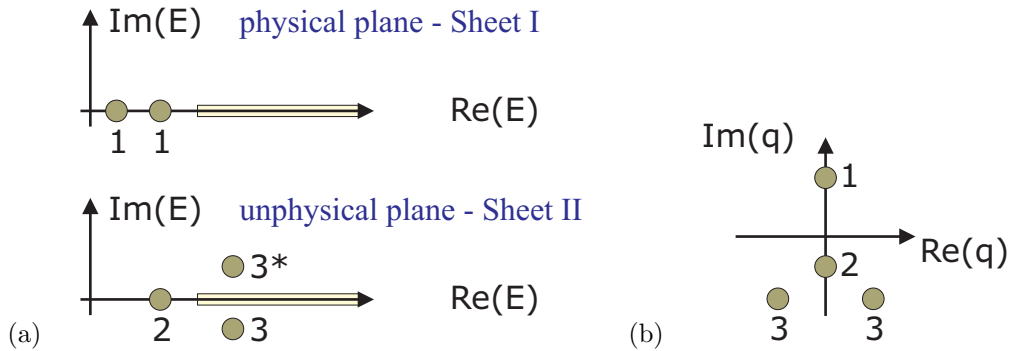


Fig. 19. – Singularities in the (a) complex energy and (b) momentum plane. (1) bound states, (2) anti-bound states and (3) resonances.

Let's go back to poles at threshold, since they are the most complicated ones and the respective resonances remain a mystery in meson spectroscopy. If the poles are far

away from thresholds, they are no really affected by them (see fig. 20a). This is true even for the $\rho(770)$ which lies exactly between two threshold. For the a_0/f_0 at the $K\bar{K}$ threshold, the situation is more puzzling. Without thresholds, the poles on sheet II and III are usually identical and lie on top of each other. At threshold, they do not and it is important to verify that the two poles which one finds near the threshold correspond to each other. A resonance can only be quoted if the poles belong to each other. Since the two sides of the threshold correspond to a different sign for ρ (sheet II: $(i\sqrt{\rho})^2 = -\rho$ and sheet III: $\sqrt{\rho}^2 = +\rho$) it is sufficient to show, that while changing ρ smoothly to $-\rho$ the poles can be connected (see fig. 20b).

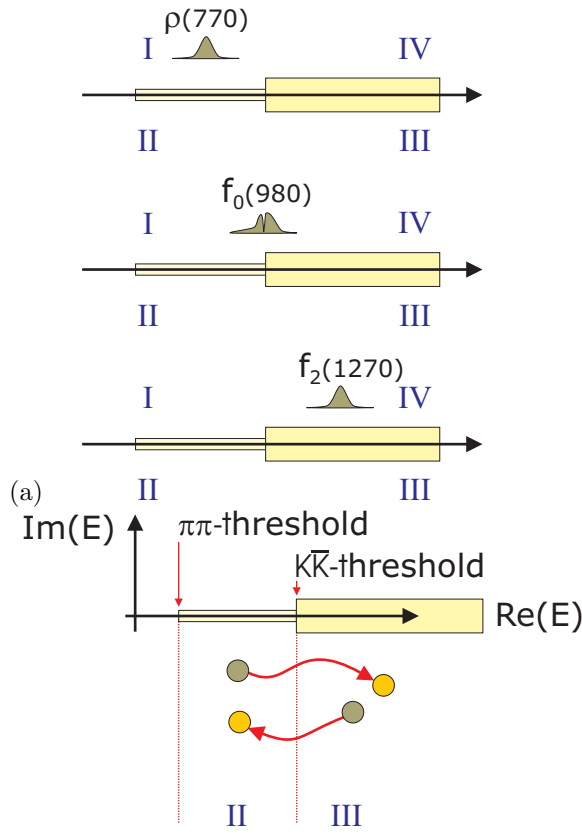


Fig. 20. – Normal poles (a,c) and shadow poles at threshold (b).

* * *

I would like to thank T. Bressani and U. Wiedner for organizing this hadron school

at such a lovely place leading to so many fruitful discussions. I also thank S.U. Chung and M.R. Pennington for teaching me a lot of the topics discussed in this primer.

In addition I would like to thank bmb+f, GSI and SIF for supporting the preparation of the lectures.

REFERENCES

- [1] PETERS K., AND KLEMP T. E., Phys. Lett. **B352** (1995) 467.
- [2] JACOB M., AND G.C. WICK, Ann. Phys.(USA) **7** (1959) 404.
- [3] KOTANSKI A., Act. Phys. Pol. **29** (1966) 699; Act. Phys. Pol. **30** (1966) 629.
- [4] CHOU K.C., AND SHIROKOV M.I., Sov. Phys. JETP **7** (1958)851.
- [5] Phys. Rev. **B1201** (1964) 133, Phys. Rev. **B97** (1965) 140, Phys. Rev. **B109** (1965) 140
- [6] DAY T.B., SNOW G.A AND SUCHER J., Phys. Rev. **118** (1960) 864.
- [7] BATTY C., Rep. Prog. Phys. **52** (1989) 1165.
- [8] PETERS K., Nucl Phys. **A692** (2001) 395c
- [9] ABELE A. ET al., Eur. J. Phys. **C8** (1999) 67.
- [10] MARTIN B.R., MORGAN D., AND SHAW G., *Pion Pion Interactions in Particle Physics*, Academic Press, 1976.
- [11] CHUNG S.U., *Spin Formalisms*, Yellow Report, CERN 71-8.
- [12] MARTIN A.D., AND SPEARMAN T.D., *Elementary Particle Theory*, North-Holland Publishing Co., Amsterdam 1970.
- [13] BURKHARDT H., *Dispersion relation dynamics*, North-Holland, Amsterdam, 1969
- [14] WIGNER E.P., Phys. Rev. **70** (1946) 15.
- [15] WIGNER E.P., AND EISENBUD L., Phys. Rev. **72** (1947) 29.
- [16] DALITZ R.H., AND TUAN S., Ann. Phys. **10** (1960) 307.
- [17] BADALYAN A.M., KOK L.P., POLIKARPOV M.I., AND SIMONOV YU.A., Phys. Rep. **82** (1982) 31.
- [18] CAHN R.N., AND LANDSHOFF P.V., Nucl. Phys. **B266** (1986) 451.
- [19] KATO M., Annals of Physics, **31** (1965) 130.
- [20] MORGAN D., AND PENNINGTON M.R., Phys. Rev. **D48** (1993) 1185.
- [21] MARTIN A.D., OZMUTLU E.N. AND SQUIRES E.J., Nucl. Phys. **B121** (1977) 514.
- [22] HIPPEL F.V. AND QUIGG C., Phys. Rev. **5** (1972) 624.
- [23] FLATTÉ S.M., Phys. Lett. **B63** (1976) 224.
- [24] AU K.L., MORGAN D. AND PENNINGTON M.R., Phys. Rev. **D35** (1987) 1633.
- [25] AMSLER C. ET al., Phys. Lett. **B355** (1995)425
- [26] ROSSELET L. ET al., Phys. Rev. **D15** (1977) 574
- [27] GRAYER G. ET al., Nucl. Phys. **B75** (1974) 189
- [28] ANISOVICH V.V., AND SARANTSEV A.V., Eur. Phys. J. **A16** 2003 229.
- [29] AITCHISON I.J.R., Nucl. Phys. **A189** (1972) 417.
- [30] WATSON K.M., Phys. Rev. **88** (1952) 1163.
- [31] LONGACRE R.S., Phys. Rev. **D26** (1982) 82
- [32] LONGACRE R.S. ET al., Phys. Lett. **B177** (1986) 223
- [33] LINDENBAUM S.J., AND LONGACRE R.S., Phys. Lett. **B274** (1992) 492
- [34] FOSTER M. ET al., Nucl. Phys. **B6** (1968) 107.
- [35] ANISOVICH V.V. ET al., Phys. Lett. **B323** (1994) 233.